



HAL
open science

Ice Giant Systems: The scientific potential of orbital missions to Uranus and Neptune

Leigh Fletcher, Ravit Helled, Elias Roussos, Geraint Jones, Sébastien Charnoz, Nicolas André, David Andrews, Michele Bannister, Emma Bunce, Thibault Cavalié, et al.

► To cite this version:

Leigh Fletcher, Ravit Helled, Elias Roussos, Geraint Jones, Sébastien Charnoz, et al.. Ice Giant Systems: The scientific potential of orbital missions to Uranus and Neptune. Planetary and Space Science, 2020, 191, pp.105030. 10.1016/j.pss.2020.105030 . hal-02969438

HAL Id: hal-02969438

<https://hal.science/hal-02969438v1>

Submitted on 4 Jan 2021

HAL is a multi-disciplinary open access archive for the deposit and dissemination of scientific research documents, whether they are published or not. The documents may come from teaching and research institutions in France or abroad, or from public or private research centers.

L'archive ouverte pluridisciplinaire **HAL**, est destinée au dépôt et à la diffusion de documents scientifiques de niveau recherche, publiés ou non, émanant des établissements d'enseignement et de recherche français ou étrangers, des laboratoires publics ou privés.

Journal Pre-proof



Ice Giant Systems: The scientific potential of orbital missions to Uranus and Neptune

Leigh N. Fletcher, Ravit Helled, Elias Roussos, Geraint Jones, Sébastien Charnoz, Nicolas André, David Andrews, Michele Bannister, Emma Bunce, Thibault Cavalié, Francesca Ferri, Jonathan Fortney, Davide Grassi, Léa Griton, Paul Hartogh, Ricardo Hueso, Yohai Kaspi, Laurent Lamy, Adam Masters, Henrik Melin, Julianne Moses, Oliver Mousis, Nadine Nettleman, Christina Plainaki, Jürgen Schmidt, Amy Simon, Gabriel Tobie, Paolo Tortora, Federico Tosi, Diego Turrini

PII: S0032-0633(20)30004-0

DOI: <https://doi.org/10.1016/j.pss.2020.105030>

Reference: PSS 105030

To appear in: *Planetary and Space Science*

Received Date: 8 January 2020

Revised Date: 12 May 2020

Accepted Date: 8 June 2020

Please cite this article as: Fletcher, L.N., Helled, R., Roussos, E., Jones, G., Charnoz, Sé., André, N., Andrews, D., Bannister, M., Bunce, E., Cavalié, T., Ferri, F., Fortney, J., Grassi, D., Griton, Lé., Hartogh, P., Hueso, R., Kaspi, Y., Lamy, L., Masters, A., Melin, H., Moses, J., Mousis, O., Nettleman, N., Plainaki, C., Schmidt, Jü., Simon, A., Tobie, G., Tortora, P., Tosi, F., Turrini, D., Ice Giant Systems: The scientific potential of orbital missions to Uranus and Neptune, *Planetary and Space Science* (2020), doi: <https://doi.org/10.1016/j.pss.2020.105030>.

This is a PDF file of an article that has undergone enhancements after acceptance, such as the addition of a cover page and metadata, and formatting for readability, but it is not yet the definitive version of record. This version will undergo additional copyediting, typesetting and review before it is published in its final form, but we are providing this version to give early visibility of the article. Please note that, during the production process, errors may be discovered which could affect the content, and all legal disclaimers that apply to the journal pertain.

© 2020 Published by Elsevier Ltd.

Ice Giant Systems:**The Scientific Potential of Orbital Missions to Uranus and Neptune**

Leigh N. Fletcher (School of Physics and Astronomy, University of Leicester, University Road, Leicester, LE1 7RH, UK; leigh.fletcher@le.ac.uk; Tel: +441162523585), **Ravit Helled** (University of Zurich, Switzerland), **Elias Roussos** (Max Planck Institute for Solar System Research, Germany), **Geraint Jones** (Mullard Space Science Laboratory, UK), **Sébastien Charnoz** (Institut de Physique du Globe de Paris, France), **Nicolas André** (Institut de Recherche en Astrophysique et Planétologie, Toulouse, France), **David Andrews** (Swedish Institute of Space Physics, Sweden), **Michele Bannister** (Queens University Belfast, UK), **Emma Bunce** (University of Leicester, UK), **Thibault Cavalié** (Laboratoire d'Astrophysique de Bordeaux, Univ. Bordeaux, CNRS, Pessac, France; LESIA, Observatoire de Paris, Université PSL, CNRS, Sorbonne Université, Univ. Paris Diderot, Sorbonne Paris Cité, Meudon, France), **Francesca Ferri** (Università degli Studi di Padova, Italy), **Jonathan Fortney** (University of Santa-Cruz, USA), **Daide Grassi** (Istituto Nazionale di AstroFisica – Istituto di Astrofisica e Planetologia Spaziali (INAF-IAPS), Rome, Italy), **Léa Griton** (Institut de Recherche en Astrophysique et Planétologie, CNRS, Toulouse, France), **Paul Hartogh** (Max-Planck-Institut für Sonnensystemforschung, Germany), **Ricardo Hueso** (Escuela de Ingeniería de Bilbao, UPV/EHU, Bilbao, Spain), **Yohai Kaspi** (Weizmann Institute of Science, Israel), **Laurent Lamy** (Observatoire de Paris, France), **Adam Masters** (Imperial College London, UK), **Henrik Melin** (University of Leicester, UK), **Julianne Moses** (Space Science Institute, USA), **Oliver Mousis** (Aix Marseille Univ, CNRS, CNES, LAM, Marseille, France), **Nadine Nettleman** (University of Rostock, Germany), **Christina Plainaki** (ASI - Italian Space Agency, Italy), **Jürgen Schmidt** (University of Oulu, Finland), **Amy Simon** (NASA Goddard Space Flight Center, USA), **Gabriel Tobie** (Université de Nantes, France), **Paolo Tortora** (Università di Bologna, Italy), **Federico Tosi** (Istituto Nazionale di AstroFisica – Istituto di Astrofisica e Planetologia Spaziali (INAF-IAPS), Rome, Italy), **Diego Turrini** (Istituto Nazionale di AstroFisica – Istituto di Astrofisica e Planetologia Spaziali (INAF-IAPS), Rome, Italy)

28 **Abstract:**

29 Uranus and Neptune, and their diverse satellite and ring systems, represent the least explored
30 environments of our Solar System, and yet may provide the archetype for the most common outcome of
31 planetary formation throughout our galaxy. Ice Giants will be the last remaining class of Solar System
32 planet to have a dedicated orbital explorer, and international efforts are under way to realise such an
33 ambitious mission in the coming decades. In 2019, the European Space Agency released a call for scientific
34 themes for its strategic science planning process for the 2030s and 2040s, known as *Voyage 2050*. We used
35 this opportunity to review our present-day knowledge of the Uranus and Neptune systems, producing a
36 revised and updated set of scientific questions and motivations for their exploration. This review article
37 describes how such a mission could explore their origins, ice-rich interiors, dynamic atmospheres, unique
38 magnetospheres, and myriad icy satellites, to address questions at the heart of modern planetary science.
39 These two worlds are superb examples of how planets with shared origins can exhibit remarkably different
40 evolutionary paths: Neptune as the archetype for Ice Giants, whereas Uranus may be atypical. Exploring
41 Uranus' natural satellites and Neptune's captured moon Triton could reveal how Ocean Worlds form and
42 remain active, redefining the extent of the habitable zone in our Solar System. For these reasons and
43 more, we advocate that an Ice Giant System explorer should become a strategic cornerstone mission within
44 ESA's *Voyage 2050* programme, in partnership with international collaborators, and targeting launch
45 opportunities in the early 2030s.

46

47 **Keywords:** Giant Planets; Ice Giants; Robotic Missions; Orbiters; Probes

48

49 1. Introduction: Why Explore Ice Giant Systems?

50 1.1 Motivations

51

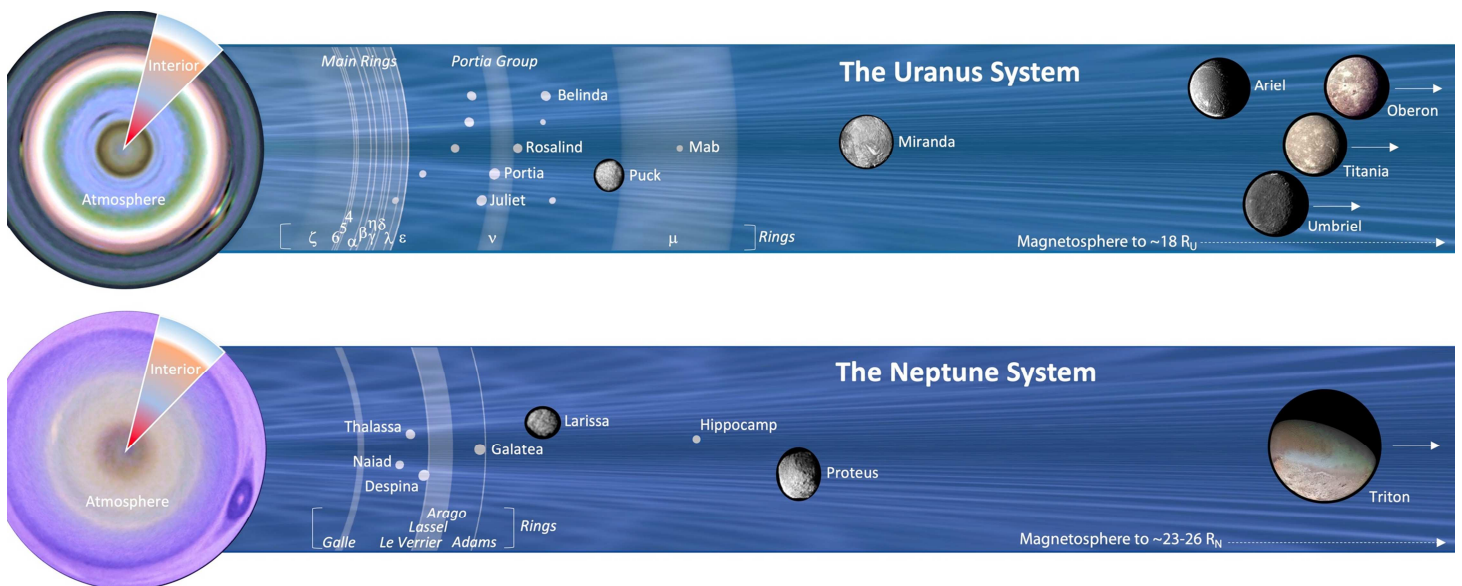


Figure 1 Each Ice Giant exhibits a rich system of planetary environments to explore, from their mysterious interiors, atmospheres and magnetospheres, to the diverse satellites and rings. The inner systems are to scale, with arrows next to major moons indicating that they orbit at larger planetocentric distances. The magnetosphere and radiation belts would encompass the full area of the figure. Credit: L.N. Fletcher/M. Hedman/E. Karkoschka/Voyager-2.

52 The early 21st century has provided unprecedented leaps in our exploration of the Gas Giant systems, via
 53 the completion of the Galileo and Cassini orbital missions at Jupiter and Saturn; NASA/Juno's ongoing
 54 exploration of Jupiter's deep interior, atmosphere, and magnetic field; ESA's development of the JUICE
 55 mission (Jupiter Icy Moons Explorer) and NASA's Europa Clipper to explore the Galilean satellites. The past
 56 decade has also provided our first glimpses of the diversity of planetary environments in the outer solar
 57 system, via the New Horizons mission to Pluto. Conversely, the realm of the Ice Giants, from Uranus (20
 58 AU) to Neptune (30 AU), remains largely unexplored, each system having been visited only once by a flyby
 59 spacecraft – Voyager 2 – in 1986 and 1989 respectively. More than three decades have passed since our
 60 first close-up glimpses of these worlds, with cameras, spectrometers and sensors based on 1960s and 70s
 61 technologies. Voyager's systems were not optimised for the Ice Giants, which were considered to be
 62 extended mission targets. Uranus and Neptune have therefore never had a dedicated mission, despite the
 63 rich and diverse systems displayed in Figure 1. A return to the Ice Giants with an orbiter is the next logical
 64 step in humankind's exploration of our Solar System.

65

66 The Ice Giants may be our closest and best representatives of a whole class of astrophysical objects, as
 67 Neptune-sized worlds have emerged as the dominant category in our expanding census of exoplanets
 68 (Fulton et al., 2018), intermediate between the smaller terrestrial worlds and the larger hydrogen-rich gas

69 giants (Section 3.3). Our own Ice Giants offer an opportunity to explore physical and chemical processes
70 within these planetary systems as the archetype for these distant exoplanets (Rymer et al., 2019).
71 Furthermore, the formation and evolution of Uranus and Neptune (Section 2.1) pose a critical test of our
72 understanding of planet formation, and of the architecture of our Solar System. Their small size, compared
73 to Jupiter, places strong constraints on the timing of planet formation. Their bulk internal composition (i.e.,
74 the fraction of rock, ices, and gases) and the differentiation with depth (i.e., molecular weight gradients,
75 phase transitions to form global water oceans and icy mantles) are poorly known, but help determine the
76 conditions and dynamics in the outer planetary nebula at the time of planet formation.

77
78 Uranus and Neptune also provide two intriguing endmembers for the Ice Giant class. Neptune may be
79 considered the archetype for a seasonal Ice Giant, whereas the cataclysmic collision responsible for Uranus'
80 extreme tilt renders it unique in our Solar System. Contrasting the conditions on these two worlds provides
81 insights into differential evolution from shared origins. The atmospheres of Uranus and Neptune (Section
82 2.2) exemplify the contrasts between these worlds. Uranus' negligible internal heat renders its atmosphere
83 extremely sluggish, with consequences for storms, meteorology, and atmospheric chemistry. Conversely,
84 Neptune's powerful winds and rapidly-evolving storms demonstrates how internal energy can drive
85 powerful weather, despite weak sunlight at 30 AU. Both of these worlds exhibit planetary banding,
86 although the atmospheric circulation responsible for these bands (and their associated winds,
87 temperatures, composition and clouds) remain unclear, and the connection to atmospheric flows below
88 the topmost clouds remains a mystery.

89
90 Conditions within the Ice Giant magnetospheres (Section 2.3) are unlike those found anywhere else, with
91 substantial offsets between their magnetic dipole axes and the planets' rotational axes implying a system
92 with an extremely unusual interaction with the solar wind and internal plasma processes, varying on both
93 rotational cycles as the planet spins, and on orbital cycles.

94

95 The diverse Ice Giant satellites (Section 2.4) and narrow, incomplete ring systems (Section 2.5) provide an
96 intriguing counterpoint to the better-studied Jovian and Saturnian systems. Uranus may feature a natural,
97 primordial satellite system with evidence of extreme and violent events (e.g., Miranda). Neptune hosts a
98 captured Kuiper Belt Object, Triton, which may itself harbour a sub-surface ocean giving rise to active
99 surface geology (e.g., south polar plumes and cryovolcanism).

100

101 Advancing our knowledge of the Ice Giants and their diverse satellite systems requires humankind's first
102 dedicated explorer for this distant realm. Such a spacecraft should combine interior science via gravity and
103 magnetic measurements, *in situ* measurements of their plasma and magnetic field environments, *in situ*
104 sampling of their chemical composition, and close-proximity multi-wavelength remote sensing of the
105 planets, their rings, and moons. This review article will summarise our present understanding of these
106 worlds, and propose a revised set of scientific questions to guide our preparation for such a mission. This
107 article is motivated by ESA's recent call for scientific themes as part of its strategic space mission planning
108 in the period from 2035 to 2050,¹ and is therefore biased to European perspectives on an Ice Giant mission,
109 as explored in the next section.

110

111 1.2 Ice Giants in ESA's Cosmic Vision

112

113 The exploration of the Ice Giants addresses themes at the heart of ESA's existing Cosmic Vision²
114 programme, namely (1) exploring the conditions for planet formation and the emergence of life; (2)
115 understanding how our solar system works; and (3) exploring the fundamental physical laws of the
116 universe. European-led concepts for Ice Giant exploration have been submitted to several ESA Cosmic
117 Vision competitions. The Uranus Pathfinder mission, an orbiting spacecraft based on heritage from Mars
118 Express and Rosetta, was proposed as a medium-class (~€0.5bn) mission in both the M3 (2010) and M4

¹ <https://www.cosmos.esa.int/web/voyage-2050>

² <http://sci.esa.int/cosmic-vision/38542-esa-br-247-cosmic-vision-space-science-for-europe-2015-2025/>

119 (2014) competitions (Arridge et al., 2012). However, the long duration of the mission, limited power
120 available, and the programmatic implications of having NASA provide the launch vehicle and radioisotope
121 thermoelectric generators (RTGs), meant that the Pathfinder concept did not proceed to the much-needed
122 Phase A study.

123

124 The importance of Ice Giant science was reinforced by multiple submissions to ESA's call for large-class
125 mission themes in 2013: a Uranus orbiter with atmospheric probe (Arridge et al., 2014), an orbiter to
126 explore Neptune and Triton (Masters et al., 2014); and a concept for dual orbiters of both worlds (Turrini et
127 al., 2014). Once again, an ice giant mission failed to proceed to the formal study phase, but ESA's Senior
128 Survey Committee (SSC³) commented that *“the exploration of the icy giants appears to be a timely
129 milestone, fully appropriate for an L class mission. The whole planetology community would be involved in
130 the various aspects of this mission... the SSC recommends that every effort is made to pursue this theme
131 through other means, such as cooperation on missions led by partner agencies.”*

132

133 This prioritisation led to collaboration between ESA and NASA in the formation of a science definition team
134 (2016-17), which looked more closely at a number of different mission architectures for a future mission to
135 the Ice Giants (Hofstadter et al., 2019). In addition, ESA's own efforts to develop nuclear power sources for
136 space applications have been progressing, with prototypes now developed to utilise the heat from the
137 decay of ²⁴¹Am as their power source (see Section 4.3), provided that the challenge of their low energy
138 density can be overcome. Such an advance might make smaller, European-led missions to the Ice Giants
139 more realistic, and addresses many of the challenges faced by the original Uranus Pathfinder concepts.

140

141 At the start of the 2020s, NASA and ESA are continuing to explore the potential for an international mission
142 to the Ice Giants. A palette of potential contributions (M-class in scale) to a US-led mission have been

³ <http://sci.esa.int/cosmic-vision/53261-report-on-science-themes-for-the-l2-and-l3-missions/>

143 identified by ESA⁴, and US scientists are currently undertaking detailed design and costing exercises for
144 missions to be assessed in the upcoming US Planetary Decadal Survey (~2022). Each of these emphasise
145 launch opportunities in the early 2030s (Section 4.2), with arrival in the early 2040s (timelines for Ice Giant
146 missions will be described in Section 4.3). This review article summarises those studies, whilst taking the
147 opportunity to update and thoroughly revise the scientific rationale for Ice Giant missions compared to
148 Arridge et al. (2012, 2014), Masters et al. (2014), Turrini et al. (2014) and Hofstadter et al. (2019). We focus
149 on the science achievable from orbit, as the science potential of in situ entry probes has been discussed
150 elsewhere (Mousis et al., 2018). Section 2 reviews our present-day knowledge of Ice Giant Systems;
151 Section 3 places the Ice Giants into their wider exoplanetary context; Section 4 briefly reviews the recent
152 mission concept studies and outstanding technological challenges; and Section 5 summarises our scientific
153 goals at the Ice Giants at the start of the 2020s.

154

155 2. Science Themes for Ice Giant Exploration

156

157 In this section we explore the five multi-disciplinary scientific themes that could be accomplished via
158 orbital exploration of the Ice Giants, and show how in-depth studies of fundamental processes at Uranus
159 and Neptune would have far-reaching implications in our Solar System and beyond. Each sub-section is
160 organised via a series of high-level questions that could form the basis of a mission traceability matrix.

161

162 2.1 Ice Giant Origins and Interiors

163

164 What does the origin, structure, and composition of the two Ice Giants reveal about the formation of
165 planetary systems? Understanding the origins and internal structures of Uranus and Neptune will
166 substantially enhance our understanding of our own Solar System and intermediate-mass exoplanets. Their

⁴ <http://sci.esa.int/future-missions-department/61307-cdf-study-report-ice-giants/>

167 bulk composition provides crucial constraints on the conditions in the solar nebula during planetary
168 formation and evolution.

169

170 ***How did the Ice Giants first form, and what constraints can be placed on the mechanisms for planetary***

171 ***accretion?*** The formation of Uranus and Neptune has been a long-standing problem for planet formation

172 theory (e.g., Pollack et al., 1996, Dodson-Robinson & Bodenheimer, 2010, Helled & Bodenheimer, 2014).

173 Yet, the large number of detected exoplanets with sizes comparable (or smaller) to that of Uranus and

174 Neptune suggests that such planetary objects are very common (e.g., Batalha et al. 2013), a fact that is in

175 conflict with theoretical calculations.

176

177 The challenge for formation models is to prevent Uranus and Neptune from accreting large amounts of

178 hydrogen-helium (H-He) gas, like the Gas Giants Jupiter and Saturn, to provide the correct final mass and

179 gas-to-solids ratios as inferred by structure **models**. In the standard planet formation model, core accretion

180 (see Helled et al., 2014 for review and the references therein), a slow planetary growth is expected to occur

181 at large radial distances where the solid surface density is lower, and the accretion rate (of planetesimals) is

182 significantly smaller. For the current locations of Uranus and Neptune, the formation timescale can be

183 comparable to the lifetimes of protoplanetary disks. Due to long accretion times at large radial distances,

184 the formation process is too slow to reach the phase of runaway gas accretion, before the gas disk

185 disappears, leaving behind an intermediate-mass planet (a failed giant planet), which consists mostly of

186 heavy elements and a small fraction of H-He gas.

187

188 However, since the total mass of H-He in both Uranus and Neptune is estimated to be 2-3 Earth masses

189 (M_{\oplus}), it implies that gas accretion had already begun, and this requires that the gas disk disappears at a

190 very specific time, to prevent further gas accretion onto the planets. This is known as the ***fine-tuning***

191 problem in Uranus/Neptune formation (e.g., Venturini & Helled, 2017). Another possibility is that Uranus

192 and Neptune formed *in situ* within a few Mys by pebble accretion. In this formation scenario, the core's

193 growth is more efficient than in the planetesimal accretion case, and the pebble isolation mass is above 20
 194 M_{\oplus} . As a result, the forming planets could be heavy-element dominated with H-He envelopes that are
 195 metal-rich due to sublimation of icy pebbles (e.g., Lambrechts et al., 2014).

196

197 Measuring the elemental abundances in the atmospheres of Uranus and Neptune can provide information
 198 on their formation history by setting limits on their formation locations and/or the type of solids
 199 (pebbles/planetesimals) that were accreted. Measurements of the elemental abundances of well-mixed
 200 noble gases, which are only accessible via *in situ* entry probes, would be particularly informative (e.g.
 201 Mousis et al., 2018). In addition, determining the atmospheric metallicity provides valuable constraints for
 202 structure models, as discussed below.

203

204 ***What is the role of giant impacts in explaining the differences between Uranus and Neptune?*** Uranus and
 205 Neptune are somewhat similar in terms of mass and radius, but they also have significant differences such
 206 as their tilt, internal heat flux, and satellite system. It is possible that these observed differences are a result
 207 of giant impacts that occurred after the formation of the planets (e.g., Safronov 1966, Stevenson 1986). An

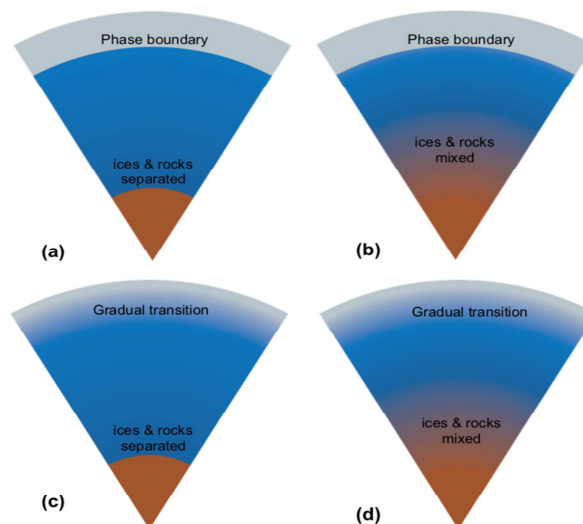


Figure 2 Sketches of the possible internal structures of the ice giants. It is unclear whether the planets are differentiated and whether the transitions between the different layers are distinct or gradual: (a) separation between the ices and rocks and the ice and H-He atmosphere (b) separation (phase boundary) between the H-He atmosphere and ices and a gradual transition between ice and rock, (c) gradual transition between the H-He atmosphere and ice layer, and a distinct separation between the ice and rock layers, and (d) gradual transition both between the H-He atmosphere and ice and the ice and rocks suggesting a global composition gradient with the planets (see text for

208 oblique impact of a massive impactor can explain Uranus' spin and lead to the formation of a disk where
209 the regular satellites form. Neptune could have also suffered a head-on impact that could have reached the
210 deep interior, providing sufficient energy (and mass) to explain the higher heat flux, and possibly the higher
211 mass and moment of inertia value (e.g., Stevenson 1986, Podolak & Helled, 2012). Giant impact simulations
212 by various groups confirmed that Uranus' tilt and rotation could be explained by a giant impact (Slattery et
213 al., 1992, Kegerreis et al., 2019). Nevertheless, alternative explanations have been proposed: Boue and
214 Laskar (2010) showed that under special circumstances, the high obliquity could potentially arise from
215 orbital migration without the need for a collision. Understanding the cause of Uranus' tilt and the
216 mechanisms that led to the observed differences between the planets are key questions in planetary
217 science.

218

219 ***What is the bulk composition and internal structure of Uranus and Neptune?*** There are still substantial
220 uncertainties regarding the bulk compositions and internal structures of Uranus and Neptune (e.g., Podolak
221 et al., 1995, Podolak & Helled, 2012, Nettelmann et al., 2013). The available measurements of their physical
222 properties such as mass, radius, rotation rate, atmospheric temperature, and gravitational and magnetic
223 fields are used to constrain models of their interiors. For the Ice Giants, only the gravitational harmonic
224 coefficients J_2 and J_4 are known and their error bars are relatively large (Jacobson, 2009; 2014),
225 nevertheless, various studies have aimed to constrain the planets' internal structures.

226

227 Standard structure models of the planets consist of three layers: a rocky core, an 'icy' shell (water,
228 ammonia, methane, etc.), and a gaseous envelope composed of H-He and heavier elements. The middle
229 layer is not made of "ice" in regard to the physical state of the material (i.e., solid), but is referred to as an
230 icy layer since it is composed of volatile materials such as water, ammonia and methane. The masses and
231 compositions of the layers are modified until the model fits the observed parameters using a physical
232 equation of state (EOS) to represent the materials. Three-layer models predict very high ice-to-rock ratios,
233 where the ice fraction is found to be higher than the rock fraction by 19-35 times for Uranus, and 4-15

234 times for Neptune, with the total H-He mass typically being 2 and 3 M_{\oplus} for Uranus and Neptune,
235 respectively. The exact estimates are highly model-dependent, and are sensitive to the assumed
236 composition, thermal structure and rotation rate of the planets (Helled et al., 2011, Nettelmann et al.,
237 2013).

238

239 The interiors of Uranus and Neptune could also be more complex with the different elements being mixed,
240 and could also include thermal boundary layers and composition gradients. Indeed, alternative structure
241 models of the planets suggested that Uranus and Neptune could have a density profile without
242 discontinuities (e.g., Helled et al., 2011), and that the planets do not need to contain large fractions of
243 water to fit their observed properties. This alternative model implies that Uranus and Neptune may not be
244 as water-rich as typically thought, but instead are rock-dominated like Pluto (e.g., McKinnon et al., 2017)
245 and could be dominated by composition gradients. It is therefore possible that the “ice giants” are in fact
246 not ice-dominated (see Helled et al., 2011 for details). The very large ice-to-rock ratios found from
247 structure models also suggest a more complex interior structure. At the moment, we have no way to
248 discriminate among the different ice-to-rock ratios inferred from structure models. As a result, further
249 constraints on the gravity and magnetic data (Section 2.3), as well as atmospheric composition and isotopic
250 ratios (e.g., D/H, Atreya et al., 2020) are required.

251

252 ***How can Ice Giant observations be used to explore the states of matter (e.g., water) and mixtures (e.g.,***
253 ***rocks, water, H-He) under the extreme conditions of planetary interiors?*** In order to predict the mixing
254 within the planets, knowledge from equation-of-state (EOS) calculations is required. Internal structure
255 models must be consistent with the phase diagram of the assumed materials and their mixtures. This is a
256 challenging task and progress in that direction is ongoing. EOS calculations can be used to guide model
257 assumptions. For example, it is possible that Uranus and Neptune have deep water oceans that begin
258 where H_2 and H_2O become insoluble (e.g., Bailey & Stevenson, 2015, Bali et al., 2013). Figure 2 presents

259 sketches of four possible internal structures of the ice giants where the transitions between layers are
260 distinct (via phase/thermal boundaries) and/or gradual.

261

262 Current observational constraints, foremost J_2 and J_4 , clearly indicate that the deep interior is more
263 enriched in heavy elements than the outer part. Understanding the nature and origin of the compositional
264 gradient zone would yield important information on the formation process and subsequent evolution
265 including possible processes such as outgassing, immiscibility, and sedimentation of ices; processes that
266 play a major role on terrestrial planets and their habitability.

267

268 ***What physical and chemical processes during the planetary formation and evolution shape the magnetic***
269 ***field, thermal profile, and other observable quantities?*** Structure models must be consistent with the
270 observed multi-polar magnetic fields (see Section 2.3), implying that the outermost ~20% of the planets is
271 convective and consists of conducting materials (e.g., Stanley & Bloxham, 2004, 2006). Currently, the best
272 candidate for the generation of the dynamo is the existence of partially dissociated fluid water in the
273 outermost layers (e.g., Redmer et al., 2011), located above solid and non-convecting superionic water ice
274 ‘mantle’ (Millot et al., 2019). Dynamo models that fit the Voyager magnetic field data suggest the deep
275 interior is stably stratified (Stanley & Bloxham 2004, 2006) or, alternatively, in a state of thermal-buoyancy
276 driven turbulent convection (Soderlund et al., 2013). Improved measurements of the magnetic fields of
277 Uranus and Neptune will also help to constrain the planetary rotation rate. Since Voyager’s measurements
278 of the periodicities in the radio emissions and magnetic fields have not been confirmed by another
279 spacecraft, it is unclear whether the Voyager rotation rate reflects the rotation of the deep interior (Helled
280 et al., 2010), with major consequences for the inferred planetary structure and the question of similar or
281 dissimilar interiors (Nettelmann et al., 2013).

282

283 Finally, the different intrinsic heat fluxes of Uranus and Neptune imply that they followed different
284 evolutionary histories. This could be a result of a different growth history or a result of giant impacts

285 during their early evolution (e.g., Reinhardt et al., 2020). Moreover, thermal evolution models that rely on
286 Voyager's measurements of the albedo, brightness temperatures, and atmospheric pressure-temperature
287 profiles that are used to model the evolution of the two planets cannot explain both planets with the same
288 set of assumptions.

289

290 **Summary: A better understanding of the origin, evolution and structure of Ice Giant planets requires**
291 **new and precise observational constraints on the planets' gravity field, rotation rate, magnetic field,**
292 **atmospheric composition, and atmospheric thermal structure, both from orbital observations and in situ**
293 **sampling from an atmospheric probe. The insights into origins, structures, dynamo operation and bulk**
294 **composition provided by an Ice Giant mission would not only shed light on the planet-forming processes**
295 **at work in our Solar System, but could also help to explain the most common planetary class throughout**
296 **our observable universe.**

297

298 2.2 Ice Giant Atmospheres

299

300 Why do atmospheric processes differ between Uranus, Neptune, and the Gas Giants, and what are the
301 implications for Neptune-mass worlds throughout our universe? Ice Giant atmospheres occupy a wholly
302 different region of parameter space compared to their Gas Giant cousins. Their dynamics and chemistry
303 are driven by extremes of internal energy (negligible on Uranus, but powerful on Neptune) and extremes of
304 solar insolation (most severe on Uranus due to its 98° axial tilt) that are not seen anywhere else in the Solar
305 System (Figure 3). Their smaller planetary radii, compared to Jupiter and Saturn, affects the width of zonal
306 bands and the drift behaviour of storms and vortices. Their zonal winds are dominated by broad
307 retrograde equatorial jets and do not exhibit the fine-scale banding found on Jupiter, which means that
308 features like bright storms and dark vortices are able to drift with latitude during their lifetimes. Their
309 hydrogen-helium atmospheres are highly enriched in volatiles like CH_4 and H_2S that show strong equator-
310 to-pole gradients, changing the atmospheric density and hence the vertical shear on the winds (Sun et al.,

311 1991). Their temperatures are so low that the energy released from interconversion between different
312 states of hydrogen (ortho and para spin isomers) can play a role in shaping atmospheric dynamics (Smith &
313 Gierasch, 1995). Their middle and upper atmospheres are both much hotter than can be explained by
314 weak solar heating alone, implying a decisive role for additional energy from internal (e.g., waves) or
315 external sources (e.g., currents induced by complex coupling to the magnetic field). As the **atmospheres**
316 **are the windows through which we interpret the bulk properties of planets**, these defining properties of
317 Ice Giants can provide insights into atmospheric processes on intermediate-sized giant planets beyond our
318 Solar System.

319

320 A combination of global multi-wavelength remote sensing from an orbiter and *in situ* measurements from
321 an entry probe would provide a transformative understanding of these unique atmospheres, focussing on
322 the following key questions (summarised in Figure 3):

323

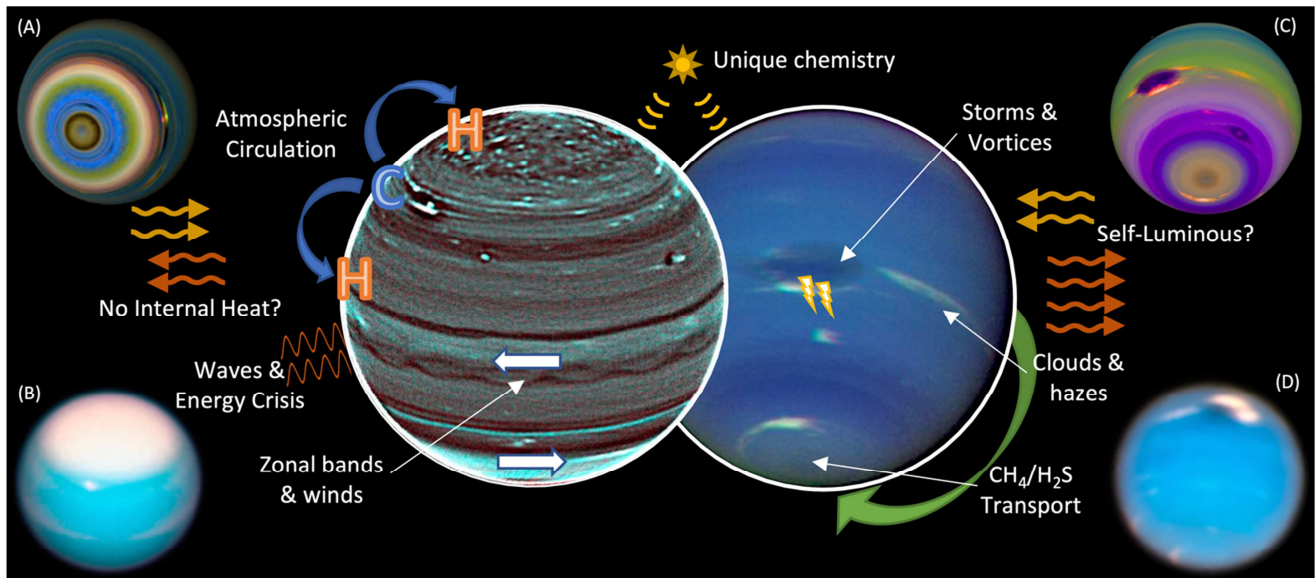


Figure 3 Ice Giant atmospheres are shaped by dynamical, chemical and radiative processes that are not found elsewhere in our Solar System. Images A & C are false-colour representations of Voyager 2 observations of Uranus and Neptune, respectively. Images B and D were acquired by the Hubble Space Telescope in 2018.

324 **What are the dynamical, meteorological, and chemical impacts of the extremes of planetary luminosity?**

325 Despite the substantial differences in self-luminosity (Pearl et al., 1990, 1991), seasonal influences,
 326 atmospheric activity (Hueso and Sanchez-Lavega et al., 2019), and the strength of vertical mixing (resulting
 327 in differences in atmospheric chemistry, Moses et al., 2018), there are many similarities between these two
 328 worlds. In their upper tropospheres, tracking of discrete cloud features has revealed that both planets
 329 exhibit broad retrograde jets at their equators and prograde jets nearer the poles (Sanchez-Lavega et al.,
 330 2018), but unlike Jupiter, these are seemingly disconnected from the fine-scale banding revealed in the
 331 visible and near-infrared (Sromovsky et al., 2015). Is this simply an observational bias, or are winds on the
 332 ice giants truly different from those on Jupiter and Saturn? What sets the scales of the bands? On the Gas
 333 Giants, small-scale eddies (from atmospheric instabilities and convective storms) appear to feed energy
 334 into the large-scale winds, but we have never been able to investigate similar processes on Uranus and
 335 Neptune. Indeed, convective processes themselves could be substantially different – moist convection
 336 driven by the condensation of water will likely play a very limited role in the observable atmosphere, as
 337 water is restricted to pressures that exceed tens or hundreds of bars. Instead, convection in the observable
 338 tropospheres may be driven by methane condensation in the 0.1-1.5 bar range (Stoker & Toon, 1989), or by
 339 heat release by ortho-para- H_2 conversion (Smith & Gierasch, 1995). These sources of energy operate in a

340 very different way compared to those available on Jupiter and Saturn. Firstly, the high enrichment in
341 methane in the Ice Giants could inhibit vertical motions due to a vertical gradient of the atmospheric
342 molecular weight (Guillot et al., 1995; Leconte et al., 2017). This phenomenon may also be at work in the
343 deep and inaccessible water clouds of both the Gas and Ice giants, but the observable methane clouds of
344 Uranus and Neptune provide an excellent opportunity to study it (Guillot et al., 2019). Secondly, heat
345 release by ortho-para H₂ conversion is much more efficient in providing energy within the cold
346 atmospheres of Uranus and Neptune. Thus, convection may occur in vertically-thin layers (Gierasch et al.,
347 1987), rather than extending vertically over tremendous heights, or in a complex and inhomogeneous
348 weather layer (Hueso et al., 2020). Multi-wavelength remote sensing of the temperatures, clouds, winds,
349 and gaseous composition is required to investigate how these meteorological processes differ from the Gas
350 Giants, how they derive their energy from the internal heating or weak sunlight, and their relation to the
351 large-scale banded patterns and winds (Fletcher et al., 2020). Spatially-resolved reflectivity and thermal-
352 emission mapping will allow precise constraints on the Ice Giant energy balance to constrain their self-
353 luminosities. And mapping the distribution and depth of Ice Giant lightning, previously detected via radio
354 emissions on both worlds (Zarka et al., 1986; Gurnett et al., 1990), could determine the frequency and
355 intensity of water-powered convection on the Ice Giants, elucidating its impact on their atmospheric
356 dynamics.

357

358 ***What is the large-scale circulation of Ice Giant atmospheres, and how deep does it go?*** Atmospheric
359 circulation, driven by both internal energy and solar heating, controls the thermal structure, radiative
360 energy balance, condensate cloud and photochemical haze characteristics, and meteorology. Unlike
361 Jupiter and Saturn, observations from Voyager, space telescopes, and ground-based observatories have
362 revealed mid-latitude upwelling (where most of the vigorous storms and coolest temperatures are found)
363 and sinking motions at the equator and poles (e.g., Conrath et al., 1998, Fletcher et al., 2020). This is
364 superimposed onto polar depletions in several key cloud-forming volatiles: methane (from reflection
365 spectroscopy, Sromovsky et al., 2014; Karkoschka et al., 2011); hydrogen sulphide (from near-IR and

366 microwave spectroscopy, de Pater et al., 1991; Hofstadter & Butler, 2003; Irwin et al., 2018); and
367 potentially ammonia (from microwave imaging). Do these contrasts imply circulation patterns extending to
368 great depths (de Pater et al., 2014), or are they restricted in vertically-thin layers (Gierasch et al., 1987)?
369 Recent re-analysis of the gravity fields measured by Voyager (Kaspi et al., 2013) suggests that zonal flows
370 are restricted to the outermost ~1000 km of their radii, indicating relatively shallow weather layers
371 overlying the deep and mysterious water-rich interiors. The circulation of the stratosphere is almost
372 entirely unknown on both worlds, due to the challenge of observing weak emissions from hydrocarbons in
373 the mid-infrared (e.g., Orton et al., 2014; Roman et al., 2020). Either way, observations of Uranus and
374 Neptune will have stark implications for atmospheric circulation on intermediate-sized planets with strong
375 chemical enrichments and latitudinal gradients.

376

377 ***How does atmospheric chemistry and haze formation respond to extreme variations in sunlight and***
378 ***vertical mixing, and the influence of external material?*** Methane can be transported into the
379 stratosphere, where photolysis initiates rich chemical pathways to produce a plethora of hydrocarbons
380 (Moses et al., 2018). The sluggish mixing of Uranus indicates that its photochemistry occurs in a different
381 physical regime (higher pressures) than on any other world. Furthermore, oxygen compounds from
382 external sources (from cometary impacts, infalling dust, satellite and ring material, Feuchtgruber et al.,
383 1997) will play different photochemical roles on Uranus, where the methane homopause is lower, than on
384 Neptune (Moses & Poppe, 2017). This exogenic influence can further complicate inferences of planetary
385 formation mechanisms from measurements of bulk abundances (particularly for CO). This rich atmospheric
386 chemistry will be substantially different from that on the Gas Giants, due to the weaker sunlight, the colder
387 temperatures (changing reaction rates and condensation processes, Moses et al., 2018), and the unusual
388 ion-neutral chemistry resulting from the complex magnetic field tilt and auroral processes (Dobrijevic et al.
389 2020). Condensation of these chemical products (and water ice) can form thin haze layers observed in
390 high-phase imaging (Rages et al., 1991), which may add to the radiative warming of the stratosphere, be
391 modulated by vertically-propagating waves, and could sediment downwards to serve as condensation

392 nuclei or aerosol coatings in the troposphere. Furthermore, Uranus' axial tilt presents an extreme test of
393 coupled chemical and transport models, given that each pole can spend decades in the shroud of winter
394 darkness. The strength of vertical mixing may vary with location, and disequilibrium tracers can be used to
395 assess where mixing is strongest (Fletcher et al., 2020; Cavalie et al., 2020). Such tracers include CO
396 (Cavalie et al., 2017), para-H₂ (Conrath et al., 1998) and yet-to-be-detected phosphine (Moreno et al.,
397 2009), arsine, germane, silane, or even tropospheric hydrocarbons (ethane, acetylene). Fluorescence
398 spectroscopy, infrared emissions and sub-mm sounding will reveal the vertical, horizontal, and temporal
399 variability of the chemical networks in the unique low-temperature regimes of Uranus and Neptune.

400

401 ***What are the sources of energy responsible for heating the middle- and upper-atmospheres?*** Weak
402 sunlight alone cannot explain the high temperatures of the stratosphere (Li et al., 2018) and thermosphere
403 (Herbert et al., 1987), and this severe deficit is known as the energy crisis. Exploration of Uranus and
404 Neptune may provide a solution to this problem, potentially revealing how waves transport energy
405 vertically from the convective troposphere into the middle atmosphere, and how the currents induced by
406 the asymmetric and time-variable magnetic fields provide energy to the upper atmosphere via Joule
407 heating. For example, the long-term cooling of Uranus' thermosphere, observed via emission from H₃⁺ in
408 the ionosphere (Melin et al., 2019), appears to follow Uranus' magnetic season, which may hint at the
409 importance of particle precipitation modulated by the magnetosphere in resolving the energy crisis.
410 Solving this issue at Uranus or Neptune, via wave observations and exploring magnetosphere-ionosphere-
411 atmosphere coupling processes (e.g., via aurora detected in the UV and infrared), will provide insights into
412 the energetics of all planetary atmospheres.

413

414 ***How do planetary ionospheres enable the energy transfer that couples the atmosphere and***
415 ***magnetosphere?*** In-situ radio occultations remain the only source for the vertical distribution of electron
416 density in the ionosphere (Majeed et al., 2004), a critical parameter for determining the strength of the
417 coupling between the atmosphere and the magnetosphere. The Voyager 2 occultations of both Uranus and

418 Neptune (Lindal et al, 1986, 1992) provided only two profiles for each planet, providing very poor
419 constraints on what drives the complex shape of the electron density profiles in the ionosphere, including
420 the influx of meteoritic material (Moses et al., 2017).

421

422 ***How do Ice Giant atmospheres change with time?*** In the decades since the Voyager encounters, Uranus
423 has displayed seasonal polar caps of reflective aerosols with changing winds (Sromovsky et al., 2015) and
424 long-term upper atmospheric changes (Melin et al., 2019); Neptune's large dark anticyclones – and their
425 associated orographic clouds – have grown, drifted, and dissipated (Lebeau et al., 1998, Stratman et al.,
426 2001, Wong et al., 2018, Simon et al., 2019); and a warm south polar vortex developed and strengthened
427 during the Neptunian summer (Fletcher et al., 2014). What are the drivers for these atmospheric changes,
428 and how do they compare to the other planets? There have been suggestions that storm activity has
429 occurred episodically, potentially with a seasonal connection (de Pater et al., 2015; Sromovsky et al., 2015),
430 but is this simply driven by observational bias to their sunlit hemispheres? Mission scenarios for the early
431 2040s would result in observations separated from those obtained by the Voyager 2 by 0.5 Uranian years
432 and 0.25 Neptunian years. Orbital remote sensing over long time periods, sampling both summer and
433 winter hemispheres, could reveal the causes of atmospheric changes in a regime of extremely weak solar
434 forcing, in contrast to Jupiter and Saturn.

435

436 **Summary:** Investigations of dynamics, chemistry, cloud formation, atmospheric circulation, and energy
437 transport on Uranus and Neptune would sample a sizeable gap in our understanding of planetary
438 atmospheres, in an underexplored regime of weak seasonal sunlight, low temperatures, and extremes of
439 internal energy and vertical mixing.

440

441 2.3 Ice Giant Magnetospheres

442

443 What can we learn about astrophysical plasma processes by studying the highly-asymmetric, fast-rotating
444 Ice Giant magnetospheres? The off-centered, oblique and fast rotating planetary magnetic fields of Uranus
445 and Neptune give rise to magnetospheres that are governed by large scale asymmetries and rapidly
446 evolving configurations (e.g. Griton et al. 2018), with no other parallels in our Solar System. The solar wind
447 that impinges upon these two magnetospheres attains Mach numbers significantly larger than those found
448 at Earth, Jupiter, and Saturn, adding further to their uniqueness (Masters et al. 2018). Magnetospheric
449 observations should thus be a high priority in the exploration of the Ice Giants because they extend the
450 sampling of the vast parameter space that controls the structure and evolution of magnetospheres, thus
451 allowing us to achieve a more universal understanding of how these systems work. Insights would also be
452 provided to astrophysical plasma processes on similar systems that are remote to us both in space and
453 time. Such may be the magnetospheres of exoplanets or even that of the Earth at times of geomagnetic
454 field reversals, when the higher order moments of the terrestrial magnetic field become significant, as
455 currently seen at the Ice Giants' (Merrill and Mcfadden, 1999). Evidence for H_3^+ ionospheric temperature
456 modulations at Uranus due to charged particle precipitation (Melin et al. 2011; 2013) is one of many
457 indications reminding us how strong a coupling between a planet and its magnetosphere can be, and why
458 the study of the latter would be essential also for achieving a system-level understanding of the Ice Giants.

459
460 A synergy between close proximity, remote sensing, and in-situ magnetospheric measurements at the Ice
461 Giants would redefine the state-of-the-art, currently determined by the single Voyager-2 flyby
462 measurements, and limited Earth-based auroral observations. Key questions that would guide such
463 observations are listed below:

464
465 ***Is there an equilibrium state of the Ice Giant magnetospheres?*** Voyager-2 spent only a few planetary
466 rotations within Uranus' and Neptune's magnetopauses, such that it was challenging to establish a nominal
467 configuration of their magnetospheres, their constituent particle populations, supporting current systems.
468 Furthermore, it is unclear whether the observations of this dynamic system represent any kind of steady

469 state, as ongoing magnetospheric reconfigurations were observed throughout each flyby, owing to the
470 large dipole tilts at the Ice Giants and their ~16 and ~17-hour rotation periods. The extent to which the two
471 magnetospheres are modified by internal plasma sources is also poorly constrained; Uranus'
472 magnetosphere for instance was observed to be devoid of any appreciable cold plasma populations
473 (McNutt et al., 1987). The presence of strong electron radiation belts (Mauk et al. 2010), seems
474 contradictory to the absence of a dense, seed population at plasma energies, or could hint an efficient local
475 acceleration process by intense wave-fields (Scarf et al. 1987). A strong proton radiation belt driven by
476 Galactic Cosmic Ray (GCR)-planet collisions may reside closer to Uranus or Neptune than Voyager-2
477 reached (e.g. Stone et al. 1986), given that Earth and Saturn, which are known to sustain such belts, are
478 exposed to a considerably lower GCR influx than the Ice Giants (Buchvarova and Belinov, 2009). Ion
479 composition and UV aurora measurements hint that Triton could be a major source of plasma in Neptune's
480 magnetosphere (Broadfoot et al., 1989, Richardson & McNutt, 1990), although questions remain as to the
481 effects of coupling between the magnetosphere and the moon's atmosphere and ionosphere in
482 establishing the plasma source (Hoogeveen & Cloutier, 1996). The magnetotails of both planets are
483 expected to have very different structures to those seen at other magnetized planets (Figure 4), with strong
484 helical magnetic field components (Cowley, 2013; Griton and Pantellini 2020), that may lead to a similarly
485 helical topology of reconnection sites across the magnetospheric current sheet (Griton et al. 2018).
486 Whether the overall magnetospheric configuration is controlled more by current sheet reconnection or a
487 viscous interaction along the magnetopause (Masters et al. 2018) is also unknown. Finally, measuring
488 average escape rates of ionospheric plasma would offer further insights on whether planetary magnetic
489 fields protect planetary atmospheres from solar wind erosion (Wei et al. 2014, Gunell et al., 2018). For such
490 dynamic systems, long-term observations that average out rotational effects and transients (e.g. Selesnick,
491 1988) are essential for achieving closure to all the aforementioned questions.

492

493 ***How do the Ice Giant magnetospheres evolve dynamically?*** The large tilts of the Ice Giant magnetic fields
494 relative to their planetary spin-axes hint that large-scale reconfigurations at diurnal time scales are

495 dominating short-term dynamics, a view supported by MHD simulations (Griton and Pantellini 2020; Griton
496 et al. 2018; Cao and Paty 2017; Mejnertsen et al. 2016). The rate of magnetic reconnection, for instance, is
497 predicted to vary strongly with rotation, and so is the rate of matter and energy transfer into the
498 magnetosphere and eventually upper atmosphere (Masters et al., 2014). Simulations do not capture how
499 such variations impact regions as the radiation belts, which would typically require a stable environment to
500 accumulate the observed, high fluxes of energetic particles (Mauk et al. 2010). A strong diurnal variability
501 may also affect the space weather conditions at the orbits of the Ice Giant moons, regulating the
502 interactions between the charged particle populations, their surfaces and exospheres (Plainaki et al., 2016;
503 Arridge et al., 2014) through processes like surface sputtering, ion pick up, and charge exchange, which
504 may also feed the magnetosphere with neutrals and low energy, heavy ion plasma (Lammer 1995). In the
505 time-frame considered here, the exploration of Neptune could provide an opportunity to study a “pole-on”
506 magnetosphere at certain rotational phases.

507

508 Additional sources of variability can be solar wind driven, such as Corotating Interaction Regions (CIRs) and
509 Interplanetary Coronal Mass Ejections (ICMEs) (Lamy et al. 2017). By the time they reach Uranus and
510 Neptune, ICMEs expand and coalesce and attain a quasi-steady radial width of $\sim 2\text{-}3$ AU (Wang and
511 Richardson, 2004) that could result in active magnetospheric episodes with week-long durations. With
512 Triton being a potential active source, Neptune’s magnetosphere may show variations at the moon’s orbital
513 period (Decker and Cheng 1994).

514

515 On longer time scales, seasonal changes of the planetary field’s orientation are most important, especially
516 at Uranus, because of its spin axis which almost lies on the ecliptic. There may be additional implications for
517 the long-term variability of the magnetosphere if magnetic field measurements reveal a secular drift of the
518 planetary field at any of the Ice Giants, in addition to providing constraints on the magnetic fields’ origin
519 and the planets’ interiors (Section 2.1).

520

521 ***How can we probe the Ice Giant magnetospheres through their aurorae?*** Aurorae form a unique
522 diagnostic of magnetospheric processes by probing the spatial distribution of active magnetospheric
523 regions and their dynamics at various timescales. Auroral emissions of Uranus and Neptune were detected
524 by Voyager 2 at ultraviolet and radio wavelengths. The Uranian UV aurora has been occasionally re-
525 detected by the Hubble Space Telescope since then. At NIR wavelengths auroral signatures remain elusive
526 (e.g. Melin et al., 2019).

527

528 UV aurora are collisionally-excited H Ly- α and H₂ band emissions from the upper atmosphere, driven by
529 precipitating energetic particles. The radical differences of the Uranian UV aurora observed across different
530 seasons were assigned to seasonal variations of the magnetosphere/solar wind interaction (Broadfoot et
531 al., 1986; Lamy et al., 2012, 2017; Cowley, 2013; Barthél my et al., 2014). The tentative detection of
532 Neptunian UV aurora did not reveal any clear planet-satellite interaction (e.g. with Triton) (Broadfoot et al.,
533 1989). Repeated UV spectro-imaging observations are essential to probe the diversity of Ice Giant aurora,
534 assess their underlying driver and constrain magnetic field models (e.g. Herbert, 2009).

535

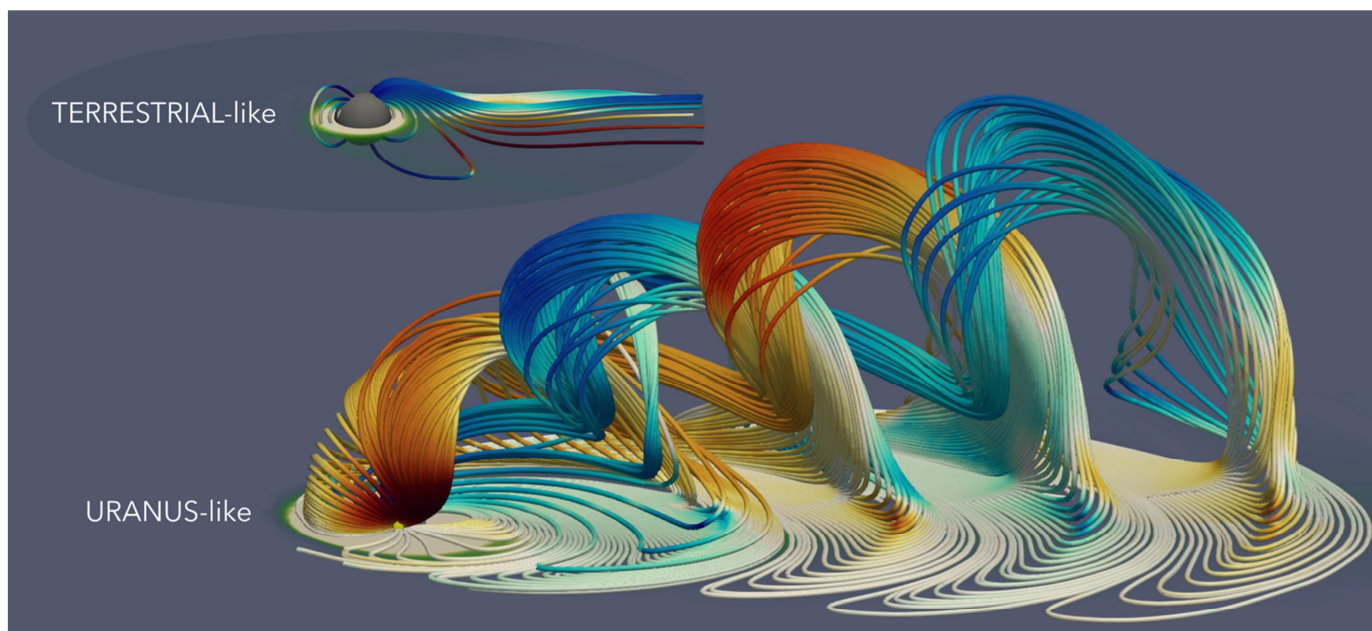


Figure 4 Typical magnetic field configuration in a terrestrial-like, solar wind driven magnetosphere (top) where the magnetic and spin axis are almost aligned, compared to a Uranus-like magnetospheric configuration (bottom), when the magnetic axis is 90° away from the spin axis, during equinox. The helicoidal magnetotail structure develops due to the planet's fast rotation.

536 Uranus and Neptune produce powerful auroral radio emissions above the ionosphere most likely driven by
537 the Cyclotron Maser Instability as at Earth, Jupiter, and Saturn. The Uranian and Neptunian Kilometric
538 Radiation are very similar (Desch et al., 1991, Zarka et al., 1995). They include (i) bursty emissions (lasting
539 for <10min) reminiscent of those from other planetary magnetospheres. A yet-to-be-identified time-
540 stationary source of free energy, able to operate in strongly variable magnetospheres, is thought to drive
541 (ii) smoother emissions (lasting for hours) that are unique in our solar system (Farrell, 1992). Long-term
542 remote and in-situ radio measurements are crucial to understand the generation of all types of Ice Giant
543 radio emissions, to complete the baseline for the search of exoplanetary radio emissions. Long-term
544 monitoring of auroral emissions will also be essential to precisely determine the rotation periods of these
545 worlds.

546

547 Summary: The Ice Giant magnetospheres comprise unique plasma physics laboratories, the study of which
548 would allow us to observe and put to test a variety of astrophysical plasma processes that cannot be
549 resolved under the conditions that prevail at the terrestrial planets and at the Gas Giants. The strong
550 planet-magnetosphere links that exist further attest to the exploration of the magnetospheres as a key
551 ingredient of the Ice Giant systems.

552

553 2.4 Ice Giant Satellites – Natural & Captured

554

555 What can a comparison of Uranus' natural satellites, the captured "Ocean World" Triton, and the myriad
556 ice-rich bodies in the Solar System, reveal about the drivers of active geology and potential habitability on
557 icy satellites? The satellite systems of Uranus and Neptune offer very different insights into moon
558 formation and evolution; they are microcosms of the larger formation and evolution of planetary systems.
559 The Neptunian system is dominated by the 'cuckoo-like' arrival of Triton (i.e., severely disrupting any
560 primordial Neptunian satellite system), which would be the largest known dwarf planet in the Kuiper belt if
561 it were still only orbiting the Sun. Neptune's remaining satellites may not be primordial, given the degree of
562 system disruption generated by Triton's arrival. In contrast, Uranus's satellite system appears to be
563 relatively undisturbed since its formation — a highly surprising situation given that Uranus has the most
564 severe axial tilt of any planet, implying a dramatic collisional event in its past. Thus, these two satellite
565 systems offer laboratories for understanding the key planetary processes of formation, capture and
566 collision.

567

568 ***What can the geological diversity of the large icy satellites of Uranus reveal about the formation and***
569 ***continued evolution of primordial satellite systems?*** The five largest moons of Uranus (Miranda, Ariel,
570 Umbriel, Titania, Oberon) are comparable in sizes and orbital configurations to the medium-sized moons of
571 Saturn. However, they have higher mean densities, about 1.5 g/cm^3 on average, and have different
572 insolation patterns: their poles are directed towards the Sun for decades at a time, due to the large axial tilt
573 of Uranus. The surfaces of Uranus's five mid-sized moons exhibit extreme geologic diversity, demonstrating
574 a complex and varied history (Figure 1). On Ariel and Miranda, signs of endogenic resurfacing associated
575 with tectonic stress, and possible cryovolcanic processes, are apparent: these moons appear to have the
576 youngest surfaces. Geological interpretation has suffered greatly from the incomplete Voyager 2 image
577 coverage of only the southern hemisphere, and extremely limited coverage by Uranus-shine in part of the

578 north (Stryk and Stooke, 2008). Apart from a very limited set of images with good resolution at Miranda,
579 revealing fascinatingly complex tectonic history and possible re-formation of the moon (Figure 5), most
580 images were acquired at low to medium resolution, only allowing characterisation of the main geological
581 units (e.g., Croft and Soderblom, 1991) and strongly limiting any surface dating from the crater-size
582 frequency distribution (e.g. Plescia, 1987a, Plescia, 1987b). High-resolution images of these moons,
583 combined with spectral data, will reveal essential information on the tectonic and cryovolcanic processes
584 and the relative ages of the different geological units, via crater statistics and sputtering processes.
585 Comparison with Saturn's inner moons system will allow us to identify key drivers in the formation and
586 evolution of compact multiplanetary systems.

587

588 ***What was the influence of tidal interaction and internal melting on shaping the Uranian worlds, and***
589 ***could internal water oceans still exist?*** As in the Jovian and Saturnian systems, tidal interaction is likely to
590 have played a key role in the evolution of the Uranian satellite system. Intense tidal heating during sporadic
591 passages through resonances is expected to have induced internal melting in some of the icy moons
592 (Titemore and Wisdom 1990). Such tidally-induced melting events, comparable to those expected on
593 Enceladus (e.g. Běhouňková et al. 2012), may have triggered the geological activity that led to the late
594 resurfacing of Ariel and possibly transient hydrothermal activity. The two largest (>1500 km diameter)
595 moons, Titania and Oberon, may still harbour liquid water oceans between their outer ice shells and inner
596 rocky cores – remnants of past melting events. Comparative study of the static and time-variable gravity
597 field of the Uranian and Saturnian moons, once well-characterized, will constrain the likelihood and
598 duration of internal melting events, essential to characterize their astrobiological potential. Complete
599 spacecraft mapping of their surfaces could reveal recent endogenic activity.

600

601 Accurate radio tracking and astrometric measurements can also be used to quantify the influence of tidal
602 interactions in the system at present, providing fundamental constraints on the dissipation factor of Uranus
603 itself (Lainey, 2008). Gravity and magnetic measurements, combined with global shape data, will greatly

604 improve the models of the satellites' interiors, providing fundamental constraints on their bulk composition
605 (density) and evolution (mean moment of inertia). Understanding their ice-to-rock ratio and internal
606 structure will enable us to understand if Uranus' natural satellite system are the original population of
607 bodies that formed around the planet, or if they were disrupted.

608

609 ***What is the chemical composition of the surfaces of the Uranian moons?*** The albedos of the major
610 Uranian moons, considerably lower than those of Saturn's moons (except Phoebe and Iapetus's dark
611 hemisphere), reveal that their surfaces are characterized by a mixture of H₂O ice and a visually dark and
612 spectrally bland material that is possibly carbonaceous in origin (Brown and Cruikshank, 1983). Pure CO₂ ice
613 is concentrated on the trailing hemispheres of Ariel, Umbriel and Titania (Grundy et al., 2006), and it
614 decreases in abundance with increasing semimajor axis (Grundy et al., 2006; Cartwright et al., 2015), as
615 opposed to what is observed in the Saturnian system. At Uranus' distance from the Sun, CO₂ ice should be
616 removed on timescales shorter than the age of the Solar System, so the detected CO₂ ice may be actively
617 produced (Cartwright et al., 2015).

618

619 The pattern of spectrally red material on the major moons will reveal their interaction with dust from the
620 decaying orbits of the irregular satellites. Spectrally red material has been detected primarily on the leading
621 hemispheres of Titania and Oberon. H₂O ice bands are stronger on the leading hemispheres of the classical
622 satellites, and the leading/trailing asymmetry in H₂O ice band strengths decreases with distance from
623 Uranus. Spectral mapping of the distribution of red material and trends in H₂O ice band strengths across
624 the satellites and rings can map out infalling dust from Uranus's inward-migrating irregular satellites
625 (Cartwright et al., 2018), similar to what is observed in the Saturnian system on Phoebe/Iapetus (e.g., Tosi
626 et al., 2010), and could reveal how coupling with the Uranus plasma and dust environment influence their
627 surface evolution.

628

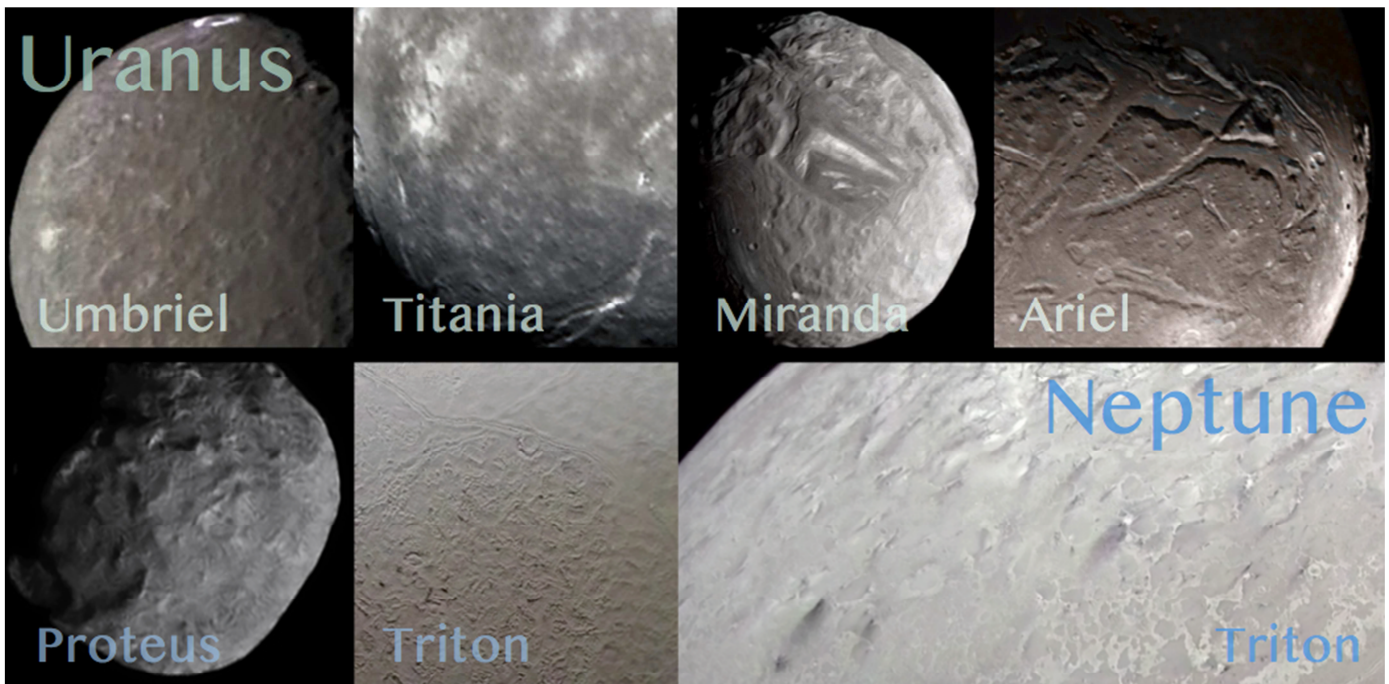


Figure 5 Best-resolution (roughly ~ 1 km/px) imagery of terrains seen in the moons of Uranus (top row) and Neptune (lower row) by Voyager 2. At Uranus, Umbriel and Titania are highly cratered with some major faults; Miranda displays spectacular and massive tectonic features; Ariel's filled-fissured surface is suggestive of late cryovolcanic activity. At Neptune, Proteus has a surface suggestive of Saturn's dust-rich moon Helene. The dwarf-planet-sized Triton has both the sublimation-related "cantaloupe terrain" (left) and active nitrogen gas geysers in the south polar terrains (right), with deposited dust visible as dark streaks. Credit: NASA/JPL-Caltech/Ted Stryk/collage M. Bannister.

629 **Does Triton currently harbour a subsurface ocean and is there evidence for recent, or ongoing, active**
 630 **exchange with its surface?** Neptune's large moon Triton, one of a rare class of Solar System bodies with a
 631 substantial atmosphere and active geology, offers a unique opportunity to study a body comparable to the
 632 dwarf planets of the rest of the trans-Neptunian region, but much closer. Triton shares many similarities in
 633 surface and atmosphere with Pluto (Grundy et al. 2016), and both may harbour current oceans. Triton's
 634 retrograde orbit indicates it was captured, causing substantial early heating. Triton, in comparison with
 635 Enceladus and Europa, will let us understand the role of tidally-induced activity on the habitability of ice-
 636 covered oceans. The major discovery of plumes emanating from the southern polar cap of Triton
 637 (Soderblom et al. 1990; see Figure 5) by Voyager 2, the most distant activity in the Solar System, is yet to be
 638 fully understood (Smith et al. 1989).

639
 640 Like Europa, Triton has a relatively young surface age of ~ 100 Ma (Stern and McKinnon 2000), inferred from
 641 its few visible impact craters. Triton also displays a variety of distinctive curvilinear ridges and associated
 642 troughs, comparable to those on Europa (Prockter et al. 2005) and especially apparent in the "cantaloupe

643 terrain". This suggests that tidal stresses and dissipation have played an essential role in Triton's geological
644 activity, and may be ongoing (Nimmo and Spencer 2015). Intense tidal heating following its capture could
645 have easily melted its icy interior (McKinnon et al. 1995). Its young surface suggests that Triton experienced
646 an ocean crystallization stage relatively recently (Hussmann et al. 2006), associated with enhanced surface
647 heat flux (Martin-Herrero et al. 2018). Combined magnetic, gravimetric and shape measurements from
648 multiple flybys or in orbit will allow us to detect if Triton possesses an ocean and to constrain the present-
649 day thickness of the ice shell. Correlating the derived shell structure and geological units will show if there
650 is exchange with the ocean. It is entirely unclear if the source(s) for Triton's plumes reaches the ocean, as at
651 Enceladus.

652

653 ***Are seasonal changes in Triton's tenuous atmosphere linked to specific sources and sinks on the surface,***
654 ***including its remarkable plume activity?*** Triton's surface has a range of volatile ices seen in Earth-based
655 near-infrared spectra, including N₂, H₂O, CO₂, and CH₄ (Quirico et al., 1999; Cruikshank et al., 2000; Tegler
656 et al, 2012). A 2.239 μm absorption feature suggests that CO and N₂ molecules are intimately mixed in the
657 ice rather than existing as separate regions of pure CO and pure N₂ deposits (Tegler et al., 2019). Mapping
658 the spatial variation of this absorption feature will constrain how the surface-atmosphere interaction
659 affects the surface composition, and more generally its climate and geologic evolution. Triton's surface may
660 also contain complex organics from atmospheric photochemistry, like those of Pluto or Saturn's moon Titan
661 (e.g. Krasnopolsky and Cruikshank 1995), as suggested by its yellowish areas (Thompson and Sagan 1990).
662 Identifying the organic compounds, and mapping out their correlation with recently active terrains and
663 geysers, will strongly raise the astrobiological potential of this exotic icy world.

664

665 Triton's tenuous atmosphere is mainly molecular nitrogen, with a trace of methane and CO near the
666 surface (Broadfoot et al. 1989, Lellouch et al. 2010). Despite Triton's distance from the Sun and its cold
667 temperatures, the weak sunlight is enough to drive strong seasonal changes on its surface and atmosphere.
668 Because CO and N₂ are the most volatile species on Triton, they are expected to dominate seasonal volatile

669 transport across its surface. Observation of increased CH₄ partial pressure between 1989 and 2010
670 (Lellouch et al. 2010) confirmed that Triton's atmosphere is seasonably variable. The plumes of nitrogen
671 gas and dust could be a seasonal solar-driven process like the CO₂ 'spiders' of the south polar regions of
672 Mars, although an endogenic origin is possible.

673

674 ***Are the smaller satellites of Neptune primordial?*** Voyager 2's flyby led to the discovery of six small moons
675 inside Triton's orbit: Naiad, Thalassa, Despina, Galatea, Larissa and Proteus. A seventh inner moon,
676 Hippocamp, has been recently discovered by HST observations orbiting between the two largest, Larissa
677 and Proteus. Almost nothing is known about these faint moons, which may post-date Triton's capture
678 rather than being primordial. Only a new space mission could unveil basic features such as shape and
679 surface composition, shedding light on their origin.

680

681 ***How does an Ice Giant satellite system interact with the planets' magnetospheres?*** Most of the major
682 moons of Uranus and Neptune orbit within the planets' extensive magnetospheres (Figure 1). The tilt and
683 offset of both planets' magnetic dipoles compared to their rotation axes mean that, unlike at Saturn, the
684 major moons at both Ice Giants experience continually-changing external magnetic fields. The potential
685 subsurface oceans of Titania, Oberon and Triton would be detectable by a spacecraft that can monitor for
686 an induced magnetic field. The moons in both systems orbit in relatively benign radiation environments,
687 but radiation belt particles could still drive sputtering processes at the inner moons' surfaces and Triton's
688 atmosphere. Triton could be a significant potential source of a neutral gas torus and magnetospheric
689 plasma at Neptune. Triton's ionosphere's transonic, sub-Alfvénic regime (Neubauer 1990; Strobel et al.
690 1990) may generate an auroral spot in Neptune's upper atmosphere. No such interaction is anticipated at
691 Uranus. Red aurorae may also be present on Triton from N₂ emission, providing valuable insights into
692 Triton's interaction with its space environment.

693

694 Summary: Exploring Uranus' and Neptune's natural satellites, as well as Neptune's captured moon Triton,
695 will reveal how ocean worlds may form and remain active, defining the extent of the habitable zone in the
696 Solar System. Both satellite systems are equally compelling for future orbital exploration.

697

698 2.5 Ice Giant Ring Systems

699

700 What processes shape the rings of Ice Giants, and why do they differ from the extensive rings of Saturn?
701 Uranus and Neptune both possess a complex system of rings and satellites (Figure 6, see also de Pater et
702 al., 2018, Nicholson et al., 2018). The rings exhibit narrow and dense ringlets, as well as fainter but broader
703 dust components. The moons can confine the rings gravitationally, and may also serve as sources and sinks
704 for ring material. Observations indicate rapid variability in the Uranian and Neptunian rings within decades.
705 A mission to the Ice Giants, with a dedicated suite of instruments, can answer fundamental questions on
706 the formation and evolution of the ring systems and the planets themselves:

707

708 ***What is the origin of the solar system ring systems, and why are they so different?*** The origin of the giant
709 planets' rings is one of the unsolved mysteries in planetary science. Whereas all four giant planets do have
710 rings, their diversity of structure and composition argues for different formation scenarios (Charnoz et al.,
711 2018). It was hypothesized that the very massive Saturnian rings formed more than 3 Gyrs ago through
712 tidal destruction of a moon, or of a body on a path traversing the system. However, recent Cassini
713 measurements (Zhang et al., 2017, Kempf et al., 2018, Waite et al., 2018, less et al., 2019) argue for a
714 younger ring age. In contrast, Uranus' and Neptune's rings are far less massive and they have a different
715 structure. Compared to Saturn, their rings' albedo is much lower, favouring a parent body that was a
716 mixture of ice and dark material (silicates and possibly organics). For instance, it was suggested (Colwell
717 and Esposito, 1992, 1993) that these two ring systems could result from the periodic destruction of
718 moonlets through meteoroid bombardment, in which case most of the ringlets would be only transient
719 structures, currently in the process of re-accretion to satellites. Among the Uranian dust rings the μ ring has

720 a distinct blue spectral slope (de Pater et al. 2006). In that regard it is similar to Saturn's E ring, for which
721 the blue slope results from the narrow size distribution of its grains, formed in the cryo-volcanic activity of
722 the moon Enceladus. Although the moon Mab is embedded in the μ ring (Showalter et al, 2006) it appears
723 much too small (12km radius) to be volcanically active and create in this way the dust that forms the ring.
724 Other dust rings of Uranus exhibit a red spectral slope (de Pater et al. 2006), suggestive of dusty material
725 released in micrometeoroid impacts on atmosphere-less moons and the origin for different appearance of
726 the μ ring is unknown. Recent ground-based observations of thermal emission from the Uranian ring
727 system (Molter et al., 2019) are consistent with the idea that the rings are made up of larger particles,
728 without micron-sized dust, and that their temperatures result from low thermal inertia and/or slow
729 rotation of the particles. Clearly, more data is needed to ultimately settle the question of the origin and
730 nature of Uranus' and Neptune's rings.

731

732 ***How do the ring-moon systems evolve?*** A variety of processes govern the evolution of planetary rings,
733 many of which are also fundamental to other cosmic disks. Important for the rings are viscous transport,
734 ring-satellite interactions, the self-gravity, as well as meteoroid bombardment and cometary impacts.
735 These processes may induce rapid evolution on timescales much shorter than the rings' age. For instance,
736 the Neptune ring arcs were initially interpreted to be confined by resonances with the moon Galatea.
737 However, it was found that the arcs actually move away from the corresponding corotation sites (Dumas et
738 al., 1999, Namouni & Porco 2002) and that they evolve rapidly (de Pater et al., 2005). Also, for the Uranian
739 rings significant changes since the Voyager epoch are observed (de Pater et al., 2006, 2007). In the Uranus
740 and Neptune systems the role the moons play in sculpting the rings is even stronger than for Saturn's rings.
741 Moreover, depending on their composition, the Uranus and Neptune ring systems may even extend
742 beyond the planet's Roche Limit (Tiscareno et al., 2013). This implies that their path of evolution is different
743 from the Saturnian rings, inducing changes on more rapid timescales. Some of the edges of the Uranian
744 rings are clearly confined by known satellites and others might be confined by yet undetected moons.

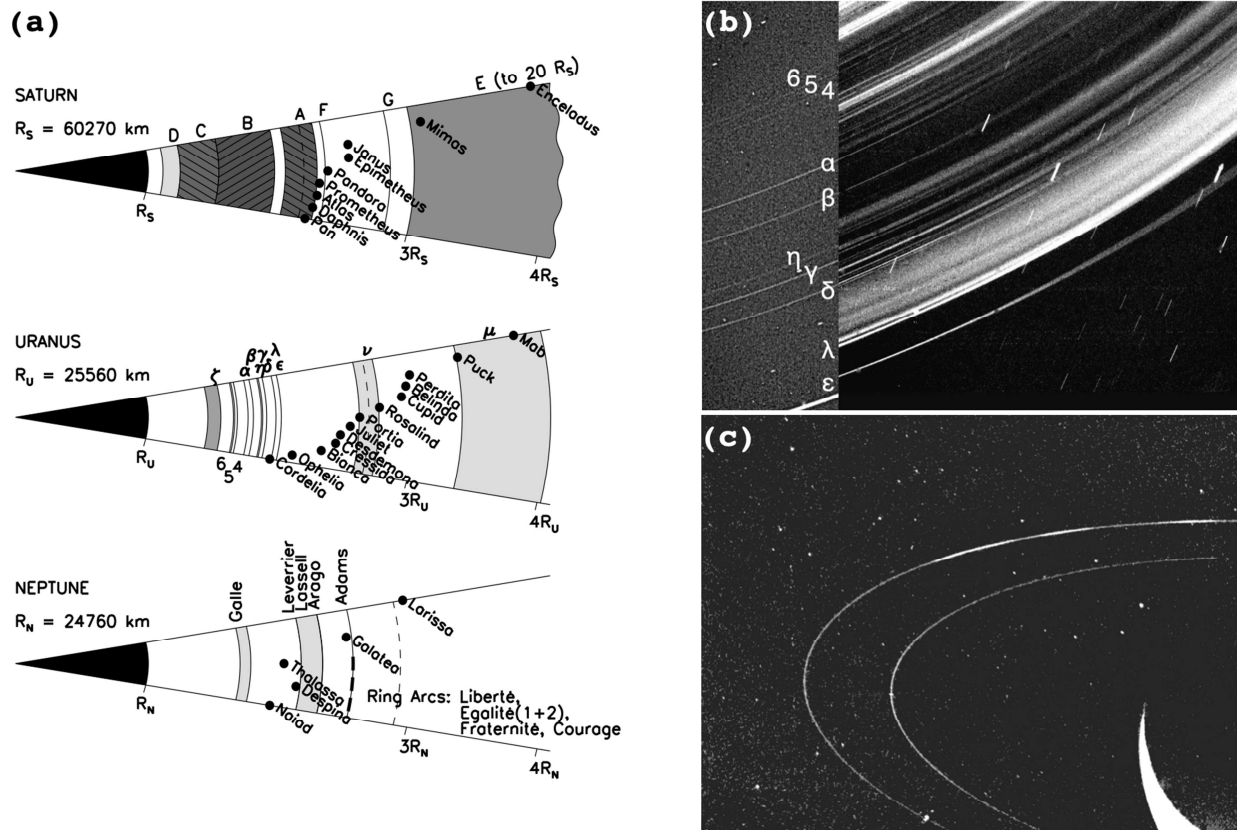


Figure 6 Panel (a): Schematic diagram of the ring moon systems of Uranus, Neptune, and Saturn for comparison. The Roche radius (for icy ring particles) is marked as a dashed line. Panel (b) shows a combination of two Voyager images of the Uranus rings, taken at low (upper part) and high (lower part) phase angle (figure from Nicholson et al., 2018). At high phase angle the dusty components of the ring system stand out. Panel (c) shows a Voyager image of the rings of Neptune (Credit: NASA/JPL).

745 Alternatively, there might be different processes of confinement at work, in a similar manner as for narrow
 746 rings of Saturn, for which shepherding moons are absent. Some of the dense rings of Uranus show sub-
 747 structure the origin of which is unclear. Spacecraft investigation will answer the question if the structure is
 748 induced by resonant interaction with moons, or if it represents intrinsic modes arising from instability and
 749 self-gravity of the rings.

750

751 **What is the ring composition?** The rings (as the moons) very likely consist of material that was present at
 752 the location in the solar system where the planets themselves have formed. Therefore, the investigation of
 753 the composition of the rings, while being interesting in its own right, may also shed light on models of
 754 planet formation and migration in the solar system.

755

756 Imaging at high and intermediate phase angles will constrain the shapes and properties of known dust rings
757 and has the potential to discover new rings. Multicolour imaging at a range of phase angles will determine
758 the size distribution of the grains that form these rings. Imaging at low phase angles will probe the dense
759 rings and allow for a comprehensive search and discovery of yet unseen satellites that serve as sources for
760 ring material and that interact dynamically with the rings. Stellar occultations performed with a high-speed
761 photometer, or radio occultations, will determine the precise optical depths of the denser rings and resolve
762 their fine sub-structure (French et al., 1991). An IR spectrometer will determine the composition of the
763 dense rings. In a complementary manner a dust detector will directly determine the composition of the
764 grains forming the low optical depth dust rings (Postberg et al., 2009) and of particles lifted from the dense
765 rings (Hsu et al., 2018). A dust detector will also measure the flux and composition of interplanetary
766 particles in the outer solar system, which is a poorly known quantity of high importance for the origin and
767 evolution of the rings.

768

769 Summary: Ice Giant rings appear to be fundamentally different to those of Saturn, such that their origin,
770 evolution, composition and gravitational relationships with the icy satellites should provide key new
771 insights into the forces shaping ring systems surrounding planetary bodies.

772 3. Ice Giant Science in Context

773

774 The scientific themes highlighted in Section 2 span multiple disciplines within planetary science, and
775 address questions that touch on issues across astronomy. In this section we review how an Ice Giant
776 mission must be considered in the context of other fields and technologies that will be developing in the
777 coming decades.

778

779 3.1 Astronomical Observatories

780

781 An Ice Giant System mission would be operating in the context of world-leading new facilities on or near
782 Earth. The 2020s will see the launch of the James Webb Space Telescope, able to provide spectral maps of
783 both Ice Giants from 1-30 μm but at a moderate spatial resolution and with limited temporal coverage.
784 Earth-based observatories in the 8-10 m class provide better spatial resolution at the expense of telluric
785 obscuration. A successor to the Hubble Space Telescope, which has been the key provider of visible and UV
786 observations of the Ice Giants, has yet to become a reality, but could be operating in the 2030s. And
787 although the next generation of Earth-based observatories in the 30+m class (the ELT, TMT, GMT) will
788 provide exquisite spatial resolution, this will remain limited to atmospheric and ionospheric investigations
789 of the Earth-facing hemisphere (with some disc-averaged spectroscopy of the satellites), leaving a
790 multitude of fundamental questions unanswered.

791

792 Additionally, distant remote sensing can only study phenomena that alter the emergent spectrum –
793 meteorology, seasonal variations, and ionospheric emissions (auroral and non-auroral). This limits our
794 understanding of the underlying mechanisms and means that ground- and space-based telescopes only
795 serve a narrow subset of the Ice Giant community, and cannot address the wide-ranging goals described in
796 Section 2. Thus, there is no substitute for orbital exploration of one or both of these Ice Giant systems
797 (alongside in situ sampling of their atmospheres), but we envisage that these space missions will work in
798 synergy with the ground-based astronomy community, following successful examples of Galileo, Cassini,
799 Juno and, ultimately, JUICE and Europa Clipper. Support from Earth-based observatories, either on the
800 ground or in space, will be used to establish a temporal baseline for atmospheric changes (e.g., tracking
801 storms), provide global context for close-in observations from the orbiters, and plug any gaps in spectral
802 coverage or spectral resolution in the orbiter payload.

803

804 3.2 Heliophysics Connection

805

806 Missions to explore the Ice Giant Systems also resonate with the heliophysics community, as detailed
807 exploration of an oblique rotator can inform a universal model of magnetospheres. The panel on solar-
808 wind magnetosphere interactions of the 2013 heliophysics decadal survey⁵ identified how the
809 magnetospheres of Uranus and Neptune are fundamentally different from others in our Solar System, and
810 sought to ensure that magnetic field instruments would be guaranteed a place on outer planet missions,
811 with a strong recommendation being that NASA's heliophysics and planetary divisions partner on a Uranus
812 orbital mission. They describe how Uranus offers an example of solar wind/magnetosphere interactions
813 under strongly changing orientations over diurnal timescales. Depending on the season, the effects of solar
814 wind-magnetosphere interaction vary dramatically over the course of each day.

815

816 There is also a need to understand how the solar wind evolves beyond 10 AU (Saturn orbit), as the states of
817 solar structures travelling within the solar wind (solar wind pressure pulses) are largely unknown due to the
818 lack of observations at such large heliocentric distances (Witasse et al., 2017). The long cruise duration of a
819 mission to Uranus or Neptune provides an excellent opportunity for both heliophysics and Ice Giant
820 communities if a space weather-monitoring package that includes a magnetometer, a solar wind analyser,
821 and a radiation monitor operates continuously during the cruise phase, to understand how conditions vary
822 out to 20-30 AU over a prolonged lifetime. Moreover, the complexity of the interactions of Uranus's
823 magnetosphere with the solar wind provides an ideal testbed for the theoretical understanding of
824 planetary interactions with the solar wind, significantly expanding the parameter range over which
825 scientists can study magnetospheric structure and dynamics. The potential discoveries from its dynamo
826 generation and its variability stand to open new chapters in comparative planetary magnetospheres and
827 interiors.

828

⁵ <https://www.nap.edu/catalog/13060/solar-and-space-physics-a-science-for-a-technological-society>

829 3.3 Exoplanet & Brown Dwarf Connection

830

831 The Ice Giant System mission will occur during an explosion in our understanding of planets beyond our
832 Solar System, through ESA's Cosmic Vision missions Plato, Euclid, and ARIEL; through missions with
833 international partners like JWST and TESS; and through next-generation observatories like WFIRST, LUVOIR,
834 Origins, and HabEx. The physical and chemical processes at work within our own Solar System serve as the
835 key foundation for our understanding of those distant and unresolved worlds. Our Solar System provides
836 the only laboratory in which we can perform in-situ experiments to understand exoplanet formation,
837 composition, structure, dynamos, systems and magnetospheres. After the several highly-successful
838 missions to the Gas Giants (and the upcoming ESA/JUICE mission), dedicated exploration of the Ice Giants
839 would place those discoveries into a broader, solar-system context.

840

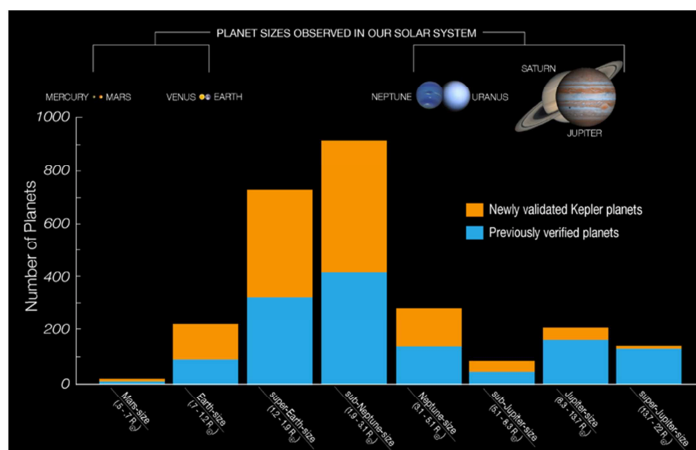


Figure 7 Known transiting exoplanets in 2016, from the Kepler mission, showing sub-Neptunes as the most common planetary radius in the current census. Credit: NASA/Ames

841 **Planet Statistics:** Uranus and Neptune represent our closest and best examples of a class of planets
 842 intermediate in mass and size between the larger, hydrogen-helium-enriched gas giants, and the rocky
 843 terrestrial worlds. Indeed, Neptune- and sub-Neptune-size worlds have emerged as commonplace in our
 844 ever-expanding census of exoplanets (Figure 7). Neptune-size planets are among the most common classes
 845 of exoplanet in our galaxy (Fulton et al., 2018). Fressin et al. (2013) suggest that this category of planets
 846 can be found around 3-31% of sun-like stars, and Petigura et al (2017) suggests that sub-Neptunes remains
 847 the most common category within Kepler's survey. Based on statistics from the Kepler mission it is
 848 predicted that TESS will detect over 1500 sub-Neptunes (2-4 R_E) over the mission (Barclay et al. 2018).
 849 Microlensing surveys (e.g., WFIRST, Penny et al., 2019) will also be more sensitive to lower-mass planets on
 850 wide orbits, and could reveal new insights into extrasolar Ice Giants ahead of a mission to Uranus or
 851 Neptune. Given these planetary occurrence rates, the exploration of bulk composition and interiors of our
 852 Ice Giants would provide strong constraints on the most common outcome for planetary formation.
 853 However, we emphasise that being Neptune-sized does not necessarily imply being Neptune-like, as a
 854 plethora of additional parameters come into play to shape the environmental conditions on these worlds.

855

856 **Atmospheric Insights:** Although we are currently unable to resolve spatial contrasts on exoplanets and
 857 brown dwarfs, comparisons of dayside (eclipse) and nightside (transit) spectra suggest the presence of
 858 powerful winds on some targets that are responsible for redistribution of energy. Brightness variations as
 859 Brown Dwarfs rotate suggest patchy cloud structures, but their rapid evolution was only understood when

860 compared with long-cadence Neptune observations (Apai et al., 2013, Stauffer et al. 2016, Simon et al.
861 2016). Changes in exoplanet transit spectra with temperature indicate complex cloud condensation
862 processes (Morley et al., 2012; Wakeford et al., 2017). Atmospheric dynamics, chemistry, and cloud
863 formation all vary as a function of planetary age, distance from the host star, and the bulk enrichments of
864 chemical species. The smaller radii of Uranus and Neptune, compared to the larger gas giants, implies
865 atmospheric processes (zonal banding, storms, vortices) at work in a different region of dynamical
866 parameter space, and one which is unavailable elsewhere in our Solar System. Detailed exploration of our
867 Ice Giants, in comparison to the existing studies of the Gas Giants, would allow us to unravel these
868 competing and complex phenomena shaping the atmospheres of exoplanets and brown dwarfs.
869 Importantly, measurements of Ice Giant composition and dynamics can be directly compared to exoplanet
870 and brown dwarf observations, placing their formation location, age, and evolution into context, and vice
871 versa. However, this cannot be done without a detailed comparative dataset from our Solar System Ice
872 Giants.

873

874 **Magnetospheric Insights:** Rymer et al. (2018) explore the importance of Ice Giant interactions with the
875 wider magnetic environment as a testbed for understanding exoplanets. Eccentric and complex orbital
876 characteristics appear commonplace beyond our Solar System, and Uranus is one of the only places where
877 radio emission, magnetospheric transport and diffusion resulting from a complex magnetospheric
878 orientation can be explored. The stability and strength of the Uranian radiation belts could also guide the
879 search for exoplanets with radiation belts. Finally, understanding the dynamos of Uranus and Neptune
880 would drastically improve our predictions of magnetic field strengths and exoplanet dynamo morphologies.
881 Each of these insights will be vital as exoplanetary science moves into an era of characterisation of
882 atmospheric composition, dynamics, clouds, and auroral/radio emissions.

883 4. Ice Giant Missions

884 4.1 Architectures: The Case for Orbiters

885

886 The scientific themes of Ice Giant System missions (summarised in Figure 9) are broad and challenging to
887 capture within a single mission architecture, but recent efforts by both ESA (e.g., the 2018-19 studies with
888 the Concurrent Design Facility for an M*-class mission⁶) and NASA (e.g., the 2017 Science Study Team
889 report, Hofstadter et al., 2019)⁷ have explored strategies to achieve many of the goals in Section 2. The
890 joint NASA-ESA science study team provided a detailed investigation of various combinations of flyby
891 missions, orbiters, multiple sub-satellites from a core spacecraft, satellite landers, and atmospheric probes.
892 Strategies to explore both Ice Giants with dual spacecraft have also been proposed (Turrini et al., 2014;
893 Simon et al., 2018). It was widely recognised that a flyby mission like Voyager, without any additional
894 components like an entry probe, was deemed to provide the lowest science return for the Ice Giants
895 themselves, despite their lower cost point. Without *in situ* measurements, and by providing only brief
896 snapshots of the evolving atmospheres and magnetospheres, and limited coverage of the satellites and
897 rings, a flyby could not deliver on the highest-priority science goals for an Ice Giant mission. Targeting
898 Triton as a flyby, or the inclusion of an entry probe, would increase the scientific reach, but would still
899 prove inadequate for whole-system science. The study found that an Ice Giant orbiter for either the
900 Uranus or Neptune systems, alongside an *in situ* atmospheric probe, would provide an unprecedented leap
901 in our understanding of these enigmatic worlds. An orbiter would maximise the time spent in the system
902 to conduct science of interest to the entire planetary community.

903
904 In our 2019 submission to ESA's call for ideas to shape the planning of space science missions in the coming
905 decades (known as Voyage 2050), we therefore proposed that an orbital mission to an Ice Giant should be
906 considered as a cornerstone of ESA's Voyage 2050 programme, if not already initiated with our
907 international partners in the coming decade. An ESA orbital mission, powered by radioisotope
908 thermoelectric generators, should be studied as an L-class mission to capitalise on the wealth of European
909 experience of the Cassini and JUICE missions. Alternatively, an M-class Ice Giant budget would allow a

⁶ <http://sci.esa.int/future-missions-department/61307-cdf-study-report-ice-giants/>

⁷ <https://www.lpi.usra.edu/icegiants/>

910 crucial contribution to an orbital mission led by our international partners. The mass and mission
911 requirements associated with additional components, such as satellite landers, *in situ* probes, or secondary
912 small satellites, must be tensioned against the capabilities of the core payload, and the capability of the
913 launch vehicle and propulsion. In all of these cases, a formal study of the requirements and capabilities is
914 necessary to mature the concept.

915

916 **Payload Considerations:** The 2017 NASA study found that payload masses of 90-150 kg could deliver
917 significant scientific return for a flagship-class mission, whilst the 2018 ESA CDF study identified 100 kg as a
918 realistic payload mass for a European orbiter. Different studies have resulted in different prioritisations for
919 instrumentation, but produced suites of orbiter experiments in common categories. Multi-spectral remote
920 sensing is required, using both imaging and spectroscopy, spanning the UV, visible, near-IR (e.g.,
921 atmosphere/surface reflectivity, dynamics; auroral observations), mid-IR, sub-mm, to centimetre
922 wavelengths (e.g., thermal emission and energy balance, atmospheric circulation). Such remote sensing is
923 also a requirement for characterising any atmospheric probe entry sites, or satellite lander sites. Direct
924 sensing of the magnetospheric and plasma environment would be accomplished via magnetometers, dust
925 detectors, plasma instruments, radio wave detectors, and potentially mass spectrometers. Radio science
926 would provide opportunities for interior sounding and neutral/ionospheric occultation studies. The
927 provision of such instruments would capitalise on European heritage on Cassini, JUICE, Rosetta,
928 Venus/Mars Express, and BepiColombo, but at the same time recognising the need to develop smaller,
929 lighter, and less power/data-intensive instruments, raising and maturing their technological readiness.

930

931 **Orbit Considerations:** Orbital missions to both Uranus and Neptune depend crucially on the chemical fuel
932 required for orbit insertion, which determines the deliverable mass. The potential use of aerocapture,
933 using atmospheric drag to slow down the spacecraft, permits larger payloads and faster trip times at the
934 expense of increased risk, which needs significant further study. Mission requirements and orbital
935 geometries will determine the inclination of orbital insertion – high geographical latitudes would benefit

936 some atmospheric, rings, and magnetospheric science, but satellite gravity assists and subsequent
937 trajectory corrections would be needed for exploration of the satellites, rings and atmosphere from a low-
938 inclination orbit. High inclinations are easier to achieve at Uranus, although Triton can be used to drive a
939 satellite tour at Neptune. The delivery and telemetry for an atmospheric entry probe must also be
940 considered in an orbital tour design (e.g., Simon et al., 2020). We also propose that distinct phases of an
941 orbital tour be considered, balancing moderate orbital distances (for remote sensing, outer magnetosphere
942 science, and a satellite tour) with close-in final orbits (for gravity science and inner magnetosphere),
943 following the example of Cassini and Juno. Multiple close flybys of major satellites are desirable to map
944 their interiors, surfaces, and atmospheres via a variety of techniques. Finally, multi-year orbital tours (at
945 least ~ 3 years) would maximise our time in the system, permitting the study of atmospheric and
946 magnetospheric changes over longer time periods. The 2018 ESA CDF study confirmed the feasibility of
947 orbital tours satisfying these scientific requirements.

948

949 **Ring Hazards:** The 2017 NASA-ESA report highlighted potentially unknown ring-plane hazards as a topic for
950 future study. Orbit insertion should be as close to the planet as possible to reduce the required fuel, but
951 the properties of Ice Giant rings remain poorly constrained. Potential options to mitigate this risk include:
952 having the insertion be further out (requiring more fuel); fly through the ring plane at an altitude where
953 atmospheric drag is high enough to reduce the number of particles, but not enough to adversely affect the
954 spacecraft; use a pathfinder spacecraft to measure the particle density ahead of time; or use Earth-based
955 observations to constrain the upper atmosphere/ring hazard. Detailed calculations on the location of this
956 safe zone are required.

957

958 4.2 Timeliness and Launch Opportunities

959

960 Trajectories to reach the Ice Giants depend on a number of factors: the use of chemical and/or solar-
961 electric propulsion (SEP) technologies; the lift capacity of the launch vehicle; the use of

962 aerocapture/aerobraking; and the need for gravity assists. The availability of Jupiter, as the largest planet,
963 is key to optimal launch trajectories, and the early 2030s offer the best opportunities. The synodic periods
964 of Uranus and Neptune with respect to Jupiter are ~ 13.8 and ~ 12.8 years, respectively, meaning that
965 optimal Jupiter gravity-assist (GA) windows occur every 13-14 years. The NASA-ESA joint study team
966 identified chemical-propulsion opportunities with a Jupiter GA in 2029-30 for Neptune, and a wider window
967 of 2030-34 for Uranus. Such windows would repeat in the 2040s, and a wider trade space (including the
968 potential to use Saturn GA or direct trajectories using the next generation of launch vehicles) should be
969 explored. We stress that a mission to an Ice Giant is feasible using conventional chemical propulsion.

970
971 Furthermore, a mission launched to Uranus or Neptune could offer significant opportunities for flybys of
972 Solar System objects en route, especially Centaurs, which are small bodies that orbit in the giant planet
973 region. This population has yet to be explored by spacecraft, but represents an important evolutionary step
974 between Kuiper Belt objects and comets. Around 300 are currently known, with 10% of these observed to
975 show cometary activity. In addition, we can expect to discover at least an order of magnitude more
976 Centaurs by the 2030s, following discoveries by the Large Synoptic Survey Telescope, increasing the
977 probability that a suitable flyby target can be found near to the trajectory to Uranus/Neptune. Some of the
978 largest of the Centaurs (~ 100 km scale objects) have their own ring systems, the origin of which has yet to
979 be explained, while smaller ones (1-10 km scale) could add an important 'pre-activity' view to better
980 interpret data from Rosetta's exploration of a comet. The payload options described in Section 4 would be
981 well suited to characterise a Centaur during a flyby.

982
983 The launch time necessarily influences the arrival time, as depicted in Figure 8. Uranus will reach northern
984 summer solstice in 2030, and northern autumnal equinox in 2050. Voyager 2 observed near northern
985 winter solstice, meaning that the north poles of the planet and satellites were shrouded in darkness. These
986 completely unexplored northern terrains will begin to disappear into darkness again in 2050, where they
987 will remain hidden for the following 42 years (half a Uranian year).

988

989 Neptune passed northern winter solstice in 2005, and will reach northern spring equinox in 2046. After this
 990 time, the southern hemispheres of the planet and satellites (most notably the plumes of Triton at high
 991 southern latitudes) will sink into winter darkness, meaning that the Triton plumes – if they are indeed
 992 restricted to the south – would no longer be in sunlight after ~2046, and would remain hidden for the next
 993 ~82 years (half a Neptunian year).

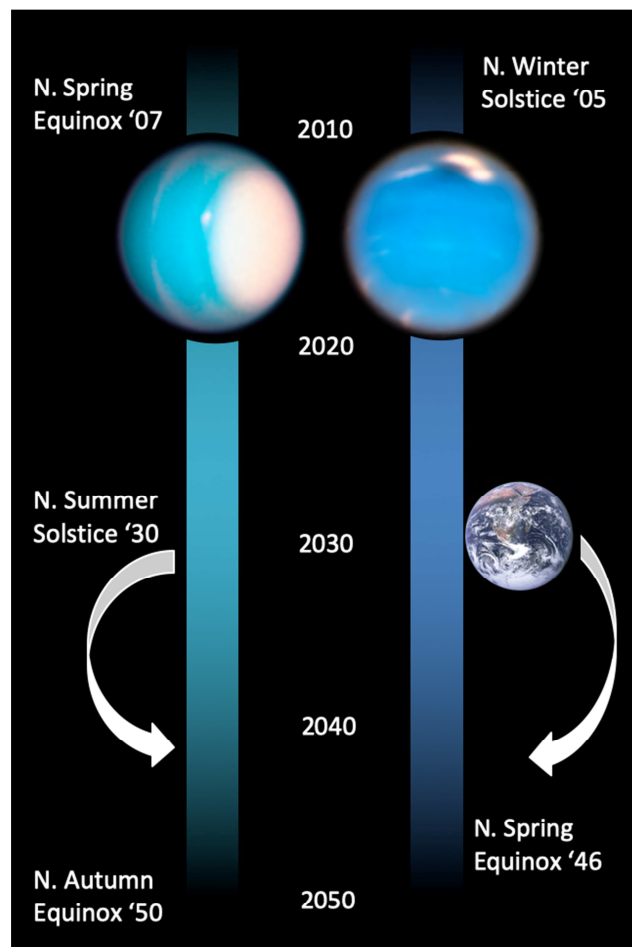


Figure 8 Potential timeline of missions to Uranus (left) and Neptune (right), compared to the seasons on each Ice Giant. The white arrows show the approximate timescales for launch opportunities in the early 2030s, with arrival in the 2040s.

994

995 The 2028-34 launch opportunities were assessed by the joint ESA-NASA study team. Saturn GA was
 996 considered but did not appear optimal for this launch window. Interplanetary flight times are 6 to 12 years
 997 to Uranus, 8 to 13 years to Neptune, depending on launch year, mission architecture, and launch vehicle.
 998 The greater challenge of reaching the Neptune system was reflected in their choice of detailed architecture

999 studies: five missions to Uranus (orbiters with/without probes; with/without SEP; and with different
1000 payload masses), and a single orbiter and probe for Neptune. Both Uranus and Neptune were deemed
1001 equally valuable as targets – Uranus standing out for its uniqueness; Neptune for the prospects of exploring
1002 Triton. The choice between these two enticing destinations will ultimately be driven by launch
1003 opportunities and deliverable mass to the systems.

1004

1005 We must capitalise on the current momentum within Europe, alongside our international partners, to make
1006 use of the launch opportunities in the ~2030s. Such a mission would arrive at Uranus while we can still see
1007 the totally-unexplored northern terrains, or at Neptune while we can still see the active geology of Triton.
1008 Operations in the 2040s would also allow ESA to maintain Outer Solar System expertise from current and
1009 future missions like JUICE. An Ice Giant explorer would therefore be active as a cornerstone of ESA's
1010 Voyage 2050 strategic planning for space missions.

1011

1012 4.3 Mature and Developing Technologies

1013

1014 An ambitious mission to an Ice Giant System would largely build on existing mature technologies (e.g., see
1015 the discussion of payload development in Section 4.1), but several challenges have been identified that, if
1016 overcome, would optimise and enhance our first dedicated orbital mission to these worlds. Note that we
1017 omit the need for ablative materials on atmospheric entry probes, which will be required for *in situ* science
1018 (Mousis et al., 2018, Simon et al., 2020). Key areas where technology maturations are required include:

1019

1020 **Space nuclear power:** With the prospect of flying solar-powered spacecraft to 20 AU being non-viable, an
1021 Ice Giant System mission must rely on radioisotope power sources, both for electricity and for spacecraft
1022 heating. In the US, existing MMRTGs (multi-mission radioisotope thermal generators), based on the decay
1023 of ^{238}Pu , will be re-designed to create eMMRTGs (“enhanced”) to increase the available specific power at
1024 the end of life, 4-5 of which were considered for the mission architectures studied in the 2017 NASA-ESA

1025 report. Previous M-class Uranus mission proposals have relied on US provision of these power sources for
1026 an ESA-led mission. However, ESA continues to pursue the development of independent power sources
1027 based on ^{241}Am (Ambrosi et al., 2019). Whilst the power density is lower than that of ^{238}Pu , the half-life is
1028 much longer, and much of the material is available from the reprocessing of spent fuel from European
1029 nuclear reactors, extracted chemically from plutonium to a ceramic oxide form. Prototypes for both
1030 radioisotope heater units (warming the spacecraft) and thermoelectric generators (providing spacecraft
1031 power) have now been demonstrated, and development is continuing for operational use late in the next
1032 decade (Ambrosi et al., 2019). An Ice Giant System mission could benefit tremendously from this
1033 independent European power source.

1034

1035 **Hardware longevity:** Given the 6- to 13-year interplanetary transfer, coupled with the desire for a long
1036 orbital tour, Ice Giant orbiters must be designed to last for a long duration under a variable thermal load
1037 imposed by gravity assists from the inner to the outer solar system. This poses constraints on the reliability
1038 of parts and power sources, as well as the need to develop optimised operational plans for the long cruise
1039 phases, such as the use of hibernation modes following the example of New Horizons.

1040

1041 **Telemetry/Communications:** All missions to the giant planets are somewhat constrained by competition
1042 between advanced instrumentation and the reduced data rates at large distances from Earth, but the case
1043 at Uranus and Neptune is most severe. The use of Ka-band in the downlink, currently supported by both
1044 the US Deep Space Network and two out of three ESA Deep Space Antennas, allows for mitigating this issue
1045 by increasing the achievable daily data volumes, but a careful optimization of the science tour remains
1046 critical. The available power, length of the downlink window, and the need to balance science data,
1047 engineering and housekeeping telemetry, all contribute to determining the overall data rate. For example,
1048 the NASA/JPL mission study⁸ in 2017 suggested that use of a 35-W traveling wave tube amplifier (the
1049 current power limit for space-qualified TWTAs) and a 34-m ground-station could provide 15 kbps at Uranus,

⁸ https://www.lpi.usra.edu/icegiants/mission_study/Full-Report.pdf

1050 whereas this could increase to 30 kbps with a 70-W TWTA. The 2018 ESA CDF study⁹ suggested that the
1051 data rate of a future M-class orbital mission to Uranus could use a 100-W TWTA to deliver 94 kbps Ka-band
1052 downlink from Uranus, or 42 kbps from Neptune. Assuming 3.2 hours/day for communications, this
1053 equates to daily data volumes for science of 1.09 and 0.48 Gb, respectively. Using current 35-W TWTAs, the
1054 ESA CDF study also suggested that lower data rates of 31 and 14 kbps could be achievable at Uranus and
1055 Neptune respectively, requiring the use of longer downlink windows. Even under the most optimistic
1056 assumptions discussed above, it is clear that some data optimization strategy would still be required. We
1057 would welcome detailed studies of new communications technologies, such as optical communications, as
1058 a general enabling technology for solar system exploration. However, we recognise that achieving the
1059 required directionality of a downlink laser from beyond 5AU will be challenging.

1060

1061 **Launch Vehicles:** The market for launch vehicles is changing dramatically both in Europe and in the US. Ice
1062 Giant mission concepts have traditionally considered Jupiter gravity assists to provide realistic flight times
1063 and sufficient payload delivered to each system. However, we also advocate investigation of the direct-
1064 transfer trajectories enabled by the heavy-lift capacity of the next generation of launch vehicles. This may
1065 (i) obviate the need for Jupiter/Saturn GA, so allow more flexibility in launch dates; and (ii) open up the
1066 possibilities for launching multiple spacecraft that share the same faring.

1067

1068 5. Summary and Perspectives

1069

1070 This article reviews and updates the scientific rationale for a mission to an Ice Giant system, advocating
1071 that an orbital mission (alongside an atmospheric entry probe, Mousis et al., 2018) be considered as a
1072 cornerstone of ESA's Voyage 2050 programme, working in collaboration with international partners to
1073 launch the *first dedicated mission* to either Uranus or Neptune. Using technologies both mature and in

⁹ <https://sci.esa.int/web/future-missions-department/-/61307-cdf-study-report-ice-giants>

1074 development, the Ice Giants community hopes to capitalise on launch opportunities in the 2030s to reach
1075 the Ice Giants. As shown in Figure 9, an Ice Giant System mission would engage a wide community,
1076 drawing expertise from a vast range of disciplines *within* planetary science, from surface geology to
1077 planetary interiors; from meteorology to ionospheric physics; from plasma scientists to heliophysicists. But
1078 this challenge is also interdisciplinary in nature, engaging those studying potentially similar Neptune-size
1079 objects beyond our Solar System, by revealing the properties of this underexplored class of planetary
1080 objects. As Neptune's orbit shapes the dynamical properties of objects in the distant solar system, an Ice
1081 Giant System mission also draws in the small-bodies community investigating objects throughout the Outer
1082 Solar System, from Centaurs, to TNOs, to Kuiper Belt Objects, and contrasting these with the natural
1083 satellites of Uranus.

1084

1085 To launch a mission to Uranus and/or Neptune in the early 2030s, the international Ice Giant community
1086 needs to significantly raise the maturity of the mission concepts and instrument technological readiness. At
1087 the time of writing (late 2019), we await the outcomes of both ESA's Voyage 2050 process, and the next US
1088 planetary decadal survey. Nevertheless, this should not delay the start of a formal science definition and
1089 study process (pre-phase A conceptual studies), so that we are ready to capitalise on any opportunities that
1090 these strategic planning surveys provide. Fully costed and technologically robust mission concepts need to
1091 be developed, studied, and ready for implementation by 2023-25 to have the potential to meet the
1092 upcoming window for Jupiter gravity assists between 2029-2034. We hope that the scientific themes and
1093 rationale identified in this review will help to guide that conceptual study process, to develop a paradigm-
1094 shifting mission that will help redefine planetary science for a generation of scientists and engineers.

1095

1096 Most importantly, the Ice Giant System mission will continue the breath-taking legacy of discovery of the
1097 Voyager, Galileo, Cassini, and Juno missions to the giant planets (in addition to the forthcoming JUICE and
1098 Europa Clipper missions). A dedicated orbiter of an Ice Giant is the next logical step in our exploration of
1099 the Solar System, completing humankind's first reconnaissance of the eight planets. It will be those

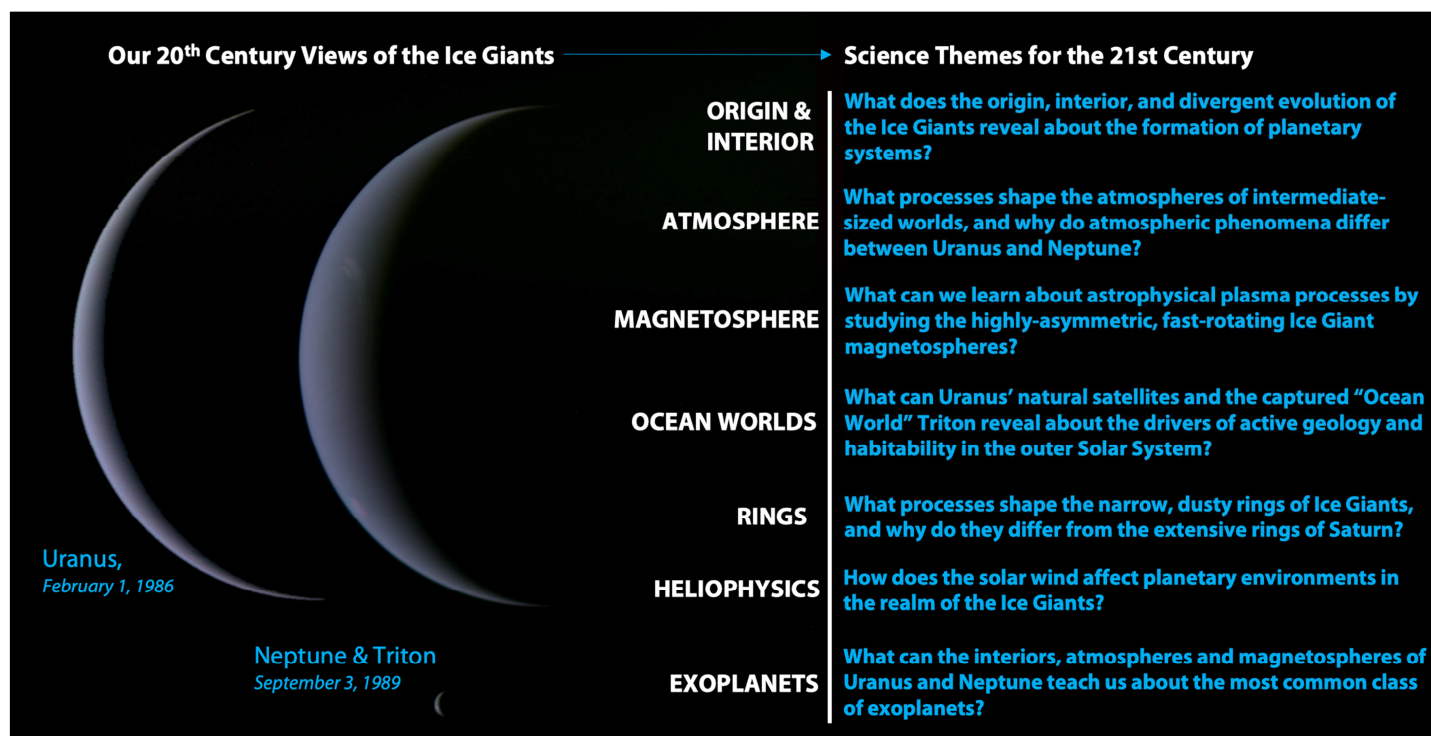


Figure 9 Left: Our last views of Uranus and Neptune from a robotic spacecraft, taken by Voyager 2 three decades ago (Credit: NASA/JPL/E. Lakdawalla). Will we see these views again before a half-century has elapsed? Right: Seven science themes for Voyage 2050 that could be addressed by an Ice Giant System mission.

1100 discoveries that no one expected, those mysteries that we did not anticipate, and those views that no
 1101 human has previously witnessed, which will enthuse the general public, and inspire the next generation of
 1102 explorers to look to the worlds of our Solar System. We urge both ESA and NASA to take up this challenge.

1103

1104

1105

1106 Acknowledgements

1107

1108 Fletcher was supported by a Royal Society Research Fellowship and European Research Council
 1109 Consolidator Grant (under the European Union's Horizon 2020 research and innovation programme, grant
 1110 agreement No 723890) at the University of Leicester. Mousis acknowledges support from CNES. Hueso was
 1111 supported by the Spanish MINECO project AYA2015-65041-P (MINECO/FEDER, UE) and by Grupos Gobierno

1112 Vasco IT1366-19 from Gobierno Vasco. UK authors acknowledge support from the Science and Technology
1113 Facilities Council (STFC). The authors are grateful to Beatriz Sanchez-Cano, Colin Snodgrass, Hannah
1114 Wakeford, Marius Millot, and Radek Poleski for their comments on early drafts of this article, and to two
1115 anonymous reviewers for their helpful suggestions. We are grateful to the members of ESA's Voyage 2050
1116 Senior Committee for allowing us to present this review at the Voyage 2050 workshop in Madrid in October
1117 2019 (see <https://www.cosmos.esa.int/web/voyage-2050/workshop-programme>).

1118

1119 References

1120 Ambrosi, R. M., Williams, H., Watkinson, E. J., et al. (2019), European Radioisotope Thermoelectric
1121 Generators (RTGs) and Radioisotope Heater Units (RHUs) for Space Science and Exploration, *Space Science*
1122 *Reviews*, 215, 55, 10.1007/s11214-019-0623-9.

1123

1124 Apai, D., Radigan, J., Buenzli, E., et al. (2013), HST Spectral Mapping of L/T Transition Brown Dwarfs Reveals
1125 Cloud Thickness Variations, *The Astrophysical Journal*, 768, 121, 10.1088/0004-637X/768/2/121.

1126

1127 Arridge, C. S., Achilleos, N., Agarwal, J., et al. (2014), The science case for an orbital mission to Uranus:
1128 Exploring the origins and evolution of ice giant planets, *Planetary and Space Science*, 104, 122,
1129 10.1016/j.pss.2014.08.009.

1130

1131 Arridge, C. S., Agnor, C. B., André, N., et al. (2012), Uranus Pathfinder: exploring the origins and evolution of
1132 Ice Giant planets, *Experimental Astronomy*, 33, 753, 10.1007/s10686-011-9251-4.

1133

1134 Atreya, S. K., Hofstadter, M. H., In, J. H., et al. (2020), Deep Atmosphere Composition, Structure, Origin, and
1135 Exploration, with Particular Focus on Critical in situ Science at the Icy Giants, *Space Science Reviews*, 216,
1136 18, 10.1007/s11214-020-0640-8.

1137

- 1138 Bailey, E., & Stevenson, D. J. (2015), Modeling Ice Giant Interiors Using Constraints on the H₂-H₂O Critical
1139 Curve, AGU Fall Meeting Abstracts, 2015, P31G-03.
1140
- 1141 Bali, E., Audéat, A., & Keppeler, H. (2013), Water and hydrogen are immiscible in Earth's mantle, *Nature*,
1142 495, 220, 10.1038/nature11908.
1143
- 1144 Barclay, T., Pepper, J., & Quintana, E. V. (2018), A Revised Exoplanet Yield from the Transiting Exoplanet
1145 Survey Satellite (TESS), *The Astrophysical Journal Supplement Series*, 239, 2, 10.3847/1538-4365/aae3e9.
1146
- 1147 Barthélemy, M., Lamy, L., Menager, H., et al. (2014), Dayglow and auroral emissions of Uranus in H₂ FUV
1148 bands, *Icarus*, 239, 160, 10.1016/j.icarus.2014.05.035.
1149
- 1150 Batalha, N. M., Rowe, J. F., Bryson, S. T., et al. (2013), Planetary Candidates Observed by Kepler. III. Analysis
1151 of the First 16 Months of Data, *The Astrophysical Journal Supplement Series*, 204, 24, 10.1088/0067-
1152 0049/204/2/24.
1153
- 1154 Běhouňková, M., Tobie, G., Choblet, G., et al. (2012), Tidally-induced melting events as the origin of south-
1155 pole activity on Enceladus, *Icarus*, 219, 655, 10.1016/j.icarus.2012.03.024.
1156
- 1157 Boué, G., & Laskar, J. (2010), A Collisionless Scenario for Uranus Tilting, *The Astrophysical Journal*, 712, L44,
1158 10.1088/2041-8205/712/1/L44.
1159
- 1160 Broadfoot, A. L., Herbert, F., Holberg, J. B., et al. (1986), Ultraviolet Spectrometer Observations of Uranus,
1161 *Science*, 233, 74, 10.1126/science.233.4759.74.
1162

- 1163 Broadfoot, A. L., Atreya, S. K., Bertaux, J. L., et al. (1989), Ultraviolet Spectrometer Observations of Neptune
1164 and Triton, *Science*, 246, 1459, 10.1126/science.246.4936.1459.
- 1165
- 1166 Brown, R. H., & Cruikshank, D. P. (1983), The Uranian satellites: Surface compositions and opposition
1167 brightness surges, *Icarus*, 55, 83, 10.1016/0019-1035(83)90052-0.
- 1168
- 1169 Buchvarova, M., & Velinov, P. (2009), Cosmic ray spectra in planetary atmospheres, *Universal Heliophysical*
1170 *Processes*, 257, 471, 10.1017/S1743921309029718.
- 1171
- 1172
- 1173 Cao, X., & Paty, C. (2017), Diurnal and seasonal variability of Uranus's magnetosphere, *Journal of*
1174 *Geophysical Research (Space Physics)*, 122, 6318, 10.1002/2017JA024063.
- 1175
- 1176 Cartwright, R. J., Emery, J. P., Rivkin, A. S., et al. (2015), Distribution of CO₂ ice on the large moons of
1177 Uranus and evidence for compositional stratification of their near-surfaces, *Icarus*, 257, 428,
1178 10.1016/j.icarus.2015.05.020.
- 1179
- 1180 Cartwright, R. J., Emery, J. P., Pinilla-Alonso, N., et al. (2018), Red material on the large moons of Uranus:
1181 Dust from the irregular satellites?, *Icarus*, 314, 210, 10.1016/j.icarus.2018.06.004.
- 1182
- 1183 Cavalié, T., Venot, O., Selsis, F., et al. (2017), Thermochemistry and vertical mixing in the tropospheres of
1184 Uranus and Neptune: How convection inhibition can affect the derivation of deep oxygen abundances,
1185 *Icarus*, 291, 1, 10.1016/j.icarus.2017.03.015.
- 1186

- 1187 Cavalié, T., Venot, O., Miguel, Y., et al. (2020), The deep composition of Uranus and Neptune from in situ
1188 exploration and thermochemical modeling, *Space Science Reviews*, accepted, 10.1007/s11214-020-00677-
1189 8.
- 1190
- 1191 Charnoz, S., Canup, R. M., Crida, A., et al. (2018), The Origin of Planetary Ring Systems, *Planetary Ring*
1192 *Systems. Properties, Structure, and Evolution*, 517, 10.1017/9781316286791.018.
- 1193
- 1194 Colwell, J. E., & Esposito, L. W. (1993), Origins of the rings of Uranus and Neptune. 2. Initial conditions and
1195 ring moon populations, *Journal of Geophysical Research*, 98, 7387, 10.1029/93JE00329.
- 1196
- 1197 Colwell, J. E., & Esposito, L. W. (1992), Origins of the rings of Uranus and Neptune 1. Statistics of satellite
1198 disruptions, *Journal of Geophysical Research*, 97, 10227, 10.1029/92JE00788.
- 1199
- 1200 Conrath, B. J., Gierasch, P. J., & Ustinov, E. A. (1998), Thermal Structure and Para Hydrogen Fraction on the
1201 Outer Planets from Voyager IRIS Measurements, *Icarus*, 135, 501, 10.1006/icar.1998.6000.
- 1202
- 1203 Cowley, S. W. H. (2013), Response of Uranus' auroras to solar wind compressions at equinox, *Journal of*
1204 *Geophysical Research (Space Physics)*, 118, 2897, 10.1002/jgra.50323.
- 1205
- 1206 Croft, S. K., & Soderblom, L. A. (1991), Geology of the Uranian satellites., *Uranus*, 561.
- 1207
- 1208 Cruikshank, D. P., Schmitt, B., Roush, T. L., et al. (2000), Water Ice on Triton, *Icarus*, 147, 309,
1209 10.1006/icar.2000.6451.
- 1210
- 1211 de Pater, I., Romani, P. N., & Atreya, S. K. (1991), Possible microwave absorption by H₂S gas in Uranus' and
1212 Neptune's atmospheres, *Icarus*, 91, 220, 10.1016/0019-1035(91)90020-T.

1213

1214 de Pater, I., Hammel, H. B., Showalter, M. R., et al. (2007), The Dark Side of the Rings of Uranus, *Science*,
1215 317, 1888, 10.1126/science.1148103.

1216

1217 de Pater, I., Sromovsky, L. A., Fry, P. M., et al. (2015), Record-breaking storm activity on Uranus in 2014,
1218 *Icarus*, 252, 121, 10.1016/j.icarus.2014.12.037.

1219

1220 de Pater, I., Gibbard, S. G., & Hammel, H. B. (2006), Evolution of the dusty rings of Uranus, *Icarus*, 180, 186,
1221 10.1016/j.icarus.2005.08.011.

1222

1223 de Pater, I., Gibbard, S. G., Chiang, E., et al. (2005), The dynamic neptunian ring arcs: evidence for a gradual
1224 disappearance of Liberté and resonant jump of courage, *Icarus*, 174, 263, 10.1016/j.icarus.2004.10.020.

1225

1226 de Pater, I., Fletcher, L. N., Luszcz-Cook, S., et al. (2014), Neptune's global circulation deduced from multi-
1227 wavelength observations, *Icarus*, 237, 211, 10.1016/j.icarus.2014.02.030.

1228

1229 de Pater, I., Renner, S., Showalter, M. R., et al. (2018), The Rings of Neptune, *Planetary Ring Systems*.
1230 Properties, Structure, and Evolution, 112, 10.1017/9781316286791.005.

1231

1232 Decker, R. B., & Cheng, A. F. (1994), A model of Triton's role in Neptune's magnetosphere, *Journal of*
1233 *Geophysical Research*, 99, 19027, 10.1029/94JE01867.

1234

1235 Desch, M. D., Kaiser, M. L., Zarka, P., et al. (1991), Uranus as a radio source., *Uranus*, 894.

1236

1237 Dobrijevic, M., Loison, J. C., Hue, V., et al. (2020), 1D photochemical model of the ionosphere and the
1238 stratosphere of Neptune, *Icarus*, 335, 113375, 10.1016/j.icarus.2019.07.009.

- 1239
- 1240 Dodson-Robinson, S. E., & Bodenheimer, P. (2010), The formation of Uranus and Neptune in solid-rich
1241 feeding zones: Connecting chemistry and dynamics, *Icarus*, 207, 491, 10.1016/j.icarus.2009.11.021.
- 1242
- 1243 Dumas, C., Terrile, R. J., Smith, B. A., et al. (1999), Stability of Neptune's ring arcs in question, *Nature*, 400,
1244 733, 10.1038/23414.
- 1245
- 1246 Farrell, W. M. (1992), Nonthermal radio emissions from Uranus, *Planetary Radio Emissions III*, 241.
- 1247
- 1248 Feuchtgruber, H., Lellouch, E., de Graauw, T., et al. (1997), External supply of oxygen to the atmospheres of
1249 the giant planets, *Nature*, 389, 159, 10.1038/38236.
- 1250
- 1251 Fletcher, L. N., de Pater, I., Orton, G. S., et al. (2020), Ice Giant Circulation Patterns: Implications for
1252 Atmospheric Probes, *Space Science Reviews*, 216, 21, 10.1007/s11214-020-00646-1.
- 1253
- 1254 Fletcher, L. N., de Pater, I., Orton, G. S., et al. (2014), Neptune at summer solstice: Zonal mean
1255 temperatures from ground-based observations, 2003-2007, *Icarus*, 231, 146, 10.1016/j.icarus.2013.11.035.
- 1256
- 1257 French, R. G., Nicholson, P. D., Porco, C. C., et al. (1991), Dynamics and structure of the Uranian rings.,
1258 *Uranus*, 327.
- 1259
- 1260 Fressin, F., Torres, G., Charbonneau, D., et al. (2013), The False Positive Rate of Kepler and the Occurrence
1261 of Planets, *The Astrophysical Journal*, 766, 81, 10.1088/0004-637X/766/2/81.
- 1262

- 1263 Fulton, B. J., & Petigura, E. A. (2018), The California-Kepler Survey. VII. Precise Planet Radii Leveraging Gaia
1264 DR2 Reveal the Stellar Mass Dependence of the Planet Radius Gap, *The Astronomical Journal*, 156, 264,
1265 10.3847/1538-3881/aae828.
- 1266
- 1267 Gierasch, P. J., & Conrath, B. J. (1987), Vertical temperature gradients on Uranus: Implications for layered
1268 convection, *Journal of Geophysical Research*, 92, 15019, 10.1029/JA092iA13p15019.
- 1269
- 1270 Griton, L., Pantellini, F., & Meliani, Z. (2018), Three-Dimensional Magnetohydrodynamic Simulations of the
1271 Solar Wind Interaction With a Hyperfast-Rotating Uranus, *Journal of Geophysical Research (Space Physics)*,
1272 123, 5394, 10.1029/2018JA025331.
- 1273
- 1274 Griton, L., & Pantellini, F. (2020), Magnetohydrodynamic simulations of a Uranus-at-equinox type rotating
1275 magnetosphere, *Astronomy and Astrophysics*, 633, A87, 10.1051/0004-6361/201936604.
- 1276
- 1277 Grundy, W. M., Binzel, R. P., Buratti, B. J., et al. (2016), Surface compositions across Pluto and Charon,
1278 *Science*, 351, aad9189, 10.1126/science.aad9189.
- 1279
- 1280 Grundy, W. M., Young, L. A., Spencer, J. R., et al. (2006), Distributions of H₂O and CO₂ ices on Ariel,
1281 Umbriel, Titania, and Oberon from IRTF/SpeX observations, *Icarus*, 184, 543, 10.1016/j.icarus.2006.04.016.
- 1282
- 1283 Guillot, T. (1995), Condensation of Methane, Ammonia, and Water and the Inhibition of Convection in
1284 Giant Planets, *Science*, 269, 1697, 10.1126/science.7569896.
- 1285
- 1286 Guillot, T. (2019), Uranus and Neptune are key to understand planets with hydrogen atmospheres, arXiv e-
1287 prints, arXiv:1908.02092.
- 1288

- 1289 Gunell, H., Maggiolo, R., Nilsson, H., et al. (2018), Why an intrinsic magnetic field does not protect a planet
1290 against atmospheric escape, *Astronomy and Astrophysics*, 614, L3, 10.1051/0004-6361/201832934.
- 1291
- 1292 Gurnett, D. A., Kurth, W. S., Cairns, I. H., et al. (1990), Whistlers in Neptune's magnetosphere: Evidence of
1293 atmospheric lightning, *Journal of Geophysical Research*, 95, 20967, 10.1029/JA095iA12p20967.
- 1294
- 1295 Helled, R., Bodenheimer, P., Podolak, M., et al. (2014), Giant Planet Formation, Evolution, and Internal
1296 Structure, *Protostars and Planets VI*, 643, 10.2458/azu_uapress_9780816531240-ch028.
- 1297
- 1298 Helled, R., & Bodenheimer, P. (2014), The Formation of Uranus and Neptune: Challenges and Implications
1299 for Intermediate-mass Exoplanets, *The Astrophysical Journal*, 789, 69, 10.1088/0004-637X/789/1/69.
- 1300
- 1301 Helled, R., Anderson, J. D., Podolak, M., et al. (2011), Interior Models of Uranus and Neptune, *The*
1302 *Astrophysical Journal*, 726, 15, 10.1088/0004-637X/726/1/15.
- 1303
- 1304 Helled, R., Anderson, J. D., & Schubert, G. (2010), Uranus and Neptune: Shape and rotation, *Icarus*, 210,
1305 446, 10.1016/j.icarus.2010.06.037.
- 1306
- 1307 Herbert, F. (2009), Aurora and magnetic field of Uranus, *Journal of Geophysical Research (Space Physics)*,
1308 114, A11206, 10.1029/2009JA014394.
- 1309
- 1310 Herbert, F., Sandel, B. R., Yelle, R. V., et al. (1987), The upper atmosphere of Uranus: EUV occultations
1311 observed by Voyager 2, *Journal of Geophysical Research*, 92, 15093, 10.1029/JA092iA13p15093.
- 1312

- 1313 Hofstadter, M., Simon, A., Atreya, S., et al. (2019), Uranus and Neptune missions: A study in advance of the
1314 next Planetary Science Decadal Survey, *Planetary and Space Science*, 177, 104680,
1315 10.1016/j.pss.2019.06.004.
- 1316
- 1317 Hofstadter, M. D., & Butler, B. J. (2003), Seasonal change in the deep atmosphere of Uranus, *Icarus*, 165,
1318 168, 10.1016/S0019-1035(03)00174-X.
- 1319
- 1320 Hoogeveen, G. W., & Cloutier, P. A. (1996), The Triton-Neptune plasma interaction, *Journal of Geophysical*
1321 *Research*, 101, 19, 10.1029/95JA02761.
- 1322
- 1323 Hsu, H.-W., Schmidt, J., Kempf, S., et al. (2018), In situ collection of dust grains falling from Saturn's rings
1324 into its atmosphere, *Science*, 362, aat3185, 10.1126/science.aat3185.
- 1325
- 1326 Hueso, R., & Sánchez-Lavega, A. (2019), Atmospheric Dynamics and Vertical Structure of Uranus and
1327 Neptune's Weather Layers, *Space Science Reviews*, 215, 52, 10.1007/s11214-019-0618-6.
- 1328
- 1329 Hueso, R., Guillot, T., Sánchez-Lavega, A. (2020). Atmospheric dynamics and convective regimes in the non-
1330 homogeneous weather layers of the ice giants, *Philosophical Transactions A*. Submitted.
- 1331
- 1332 Hussmann, H., Sohl, F., & Spohn, T. (2006), Subsurface oceans and deep interiors of medium-sized outer
1333 planet satellites and large trans-neptunian objects, *Icarus*, 185, 258, 10.1016/j.icarus.2006.06.005.
- 1334
- 1335 Iess, L., Militzer, B., Kaspi, Y., et al. (2019), Measurement and implications of Saturn's gravity field and ring
1336 mass, *Science*, 364, aat2965, 10.1126/science.aat2965.
- 1337

- 1338 Irwin, P. G. J., Toledo, D., Garland, R., et al. (2018), Detection of hydrogen sulfide above the clouds in
1339 Uranus's atmosphere, *Nature Astronomy*, 2, 420, 10.1038/s41550-018-0432-1.
- 1340
- 1341 Jacobson, R. A. (2014), The Orbits of the Uranian Satellites and Rings, the Gravity Field of the Uranian
1342 System, and the Orientation of the Pole of Uranus, *The Astronomical Journal*, 148, 76, 10.1088/0004-
1343 6256/148/5/76.
- 1344
- 1345 Jacobson, R. A. (2009), The Orbits of the Neptunian Satellites and the Orientation of the Pole of Neptune,
1346 *The Astronomical Journal*, 137, 4322, 10.1088/0004-6256/137/5/4322.
- 1347
- 1348 Karkoschka, E., & Tomasko, M. G. (2011), The haze and methane distributions on Neptune from HST-STIS
1349 spectroscopy, *Icarus*, 211, 780, 10.1016/j.icarus.2010.08.013.
- 1350
- 1351 Kaspi, Y., Showman, A. P., Hubbard, W. B., et al. (2013), Atmospheric confinement of jet streams on Uranus
1352 and Neptune, *Nature*, 497, 344, 10.1038/nature12131.
- 1353
- 1354 Kegerreis, J. A., Eke, V. R., Gonnet, P., et al. (2019), Planetary giant impacts: convergence of high-resolution
1355 simulations using efficient spherical initial conditions and SWIFT, *Monthly Notices of the Royal*
1356 *Astronomical Society*, 487, 5029, 10.1093/mnras/stz1606.
- 1357
- 1358 Kempf, S., Altobelli, N., Srama, R., et al. (2018), The Age of Saturn's Rings Constrained by the Meteoroid
1359 Flux Into the System, *EGU General Assembly Conference Abstracts*, 10791.
- 1360
- 1361 Krasnopolsky, V. A., & Cruikshank, D. P. (1995), Photochemistry of Triton's atmosphere and ionosphere.,
1362 *Journal of Geophysical Research*, 100, 21,271,286.
- 1363

- 1364 Laine, V. (2008), A new dynamical model for the Uranian satellites, *Planetary and Space Science*, 56, 1766,
1365 10.1016/j.pss.2008.02.015.
- 1366
- 1367 Lambrechts, M., Johansen, A., & Morbidelli, A. (2014), Separating gas-giant and ice-giant planets by halting
1368 pebble accretion, *Astronomy and Astrophysics*, 572, A35, 10.1051/0004-6361/201423814.
- 1369
- 1370 Lammer, H. (1995), Mass loss of N₂ molecules from Triton by magnetospheric plasma interaction,
1371 *Planetary and Space Science*, 43, 845, 10.1016/0032-0633(94)00214-C.
- 1372
- 1373 Lamy, L., Prangé, R., Hansen, K. C., et al. (2017), The aurorae of Uranus past equinox, *Journal of Geophysical*
1374 *Research (Space Physics)*, 122, 3997, 10.1002/2017JA023918.
- 1375
- 1376 Lamy, L., Prangé, R., Hansen, K. C., et al. (2012), Earth-based detection of Uranus' aurorae, *Geophysical*
1377 *Research Letters*, 39, L07105, 10.1029/2012GL051312.
- 1378
- 1379 LeBeau, R. P., & Dowling, T. E. (1998), EPIC Simulations of Time-Dependent, Three-Dimensional Vortices
1380 with Application to Neptune's Great Dark SPOT, *Icarus*, 132, 239, 10.1006/icar.1998.5918.
- 1381
- 1382 Leconte, J., Selsis, F., Hersant, F., et al. (2017), Condensation-inhibited convection in hydrogen-rich
1383 atmospheres . Stability against double-diffusive processes and thermal profiles for Jupiter, Saturn, Uranus,
1384 and Neptune, *Astronomy and Astrophysics*, 598, A98, 10.1051/0004-6361/201629140.
- 1385
- 1386 Lellouch, E., de Bergh, C., Sicardy, B., et al. (2010), Detection of CO in Triton's atmosphere and the nature of
1387 surface-atmosphere interactions, *Astronomy and Astrophysics*, 512, L8, 10.1051/0004-6361/201014339.
- 1388

- 1389 Li, C., Le, T., Zhang, X., et al. (2018), A high-performance atmospheric radiation package: With applications
1390 to the radiative energy budgets of giant planets, *Journal of Quantitative Spectroscopy and Radiative*
1391 *Transfer*, 217, 353, 10.1016/j.jqsrt.2018.06.002.
- 1392
- 1393 Lindal, G. F., Lyons, J. R., Sweetnam, D. N., et al. (1987), The atmosphere of Uranus: Results of radio
1394 occultation measurements with Voyager 2, *Journal of Geophysical Research*, 92, 14987,
1395 10.1029/JA092iA13p14987.
- 1396
- 1397 Lindal, G. F. (1992), The Atmosphere of Neptune: an Analysis of Radio Occultation Data Acquired with
1398 Voyager 2, *The Astronomical Journal*, 103, 967, 10.1086/116119.
- 1399
- 1400 Majeed, T., Waite, J. H., Bougher, S. W., et al. (2004), The ionospheres-thermospheres of the giant planets,
1401 *Advances in Space Research*, 33, 197, 10.1016/j.asr.2003.05.009.
- 1402
- 1403 Martin-Herrero, A., Romeo, I., & Ruiz, J. (2018), Heat flow in Triton: Implications for heat sources powering
1404 recent geologic activity, *Planetary and Space Science*, 160, 19, 10.1016/j.pss.2018.03.010.
- 1405
- 1406 Masters, A. (2014), Magnetic reconnection at Uranus' magnetopause, *Journal of Geophysical Research*
1407 *(Space Physics)*, 119, 5520, 10.1002/2014JA020077.
- 1408
- 1409 Masters, A. (2018), A More Viscous-Like Solar Wind Interaction With All the Giant Planets, *Geophysical*
1410 *Research Letters*, 45, 7320, 10.1029/2018GL078416.
- 1411
- 1412 Masters, A., Achilleos, N., Agnor, C. B., et al. (2014), Neptune and Triton: Essential pieces of the Solar
1413 System puzzle, *Planetary and Space Science*, 104, 108, 10.1016/j.pss.2014.05.008.
- 1414

- 1415 Mauk, B. H., & Fox, N. J. (2010), Electron radiation belts of the solar system, *Journal of Geophysical*
1416 *Research (Space Physics)*, 115, A12220, 10.1029/2010JA015660.
- 1417
- 1418 McKinnon, W. B., & Leith, A. C. (1995), Gas drag and the orbital evolution of a captured Triton., *Icarus*, 118,
1419 392, 10.1006/icar.1995.1199.
- 1420
- 1421 McKinnon, W. B., Stern, S. A., Weaver, H. A., et al. (2017), Origin of the Pluto-Charon system: Constraints
1422 from the New Horizons flyby, *Icarus*, 287, 2, 10.1016/j.icarus.2016.11.019.
- 1423
- 1424 McNutt, R. L., Selesnick, R. S., & Richardson, J. D. (1987), Low-energy plasma observations in the
1425 magnetosphere of Uranus, *Journal of Geophysical Research*, 92, 4399, 10.1029/JA092iA05p04399.
- 1426
- 1427 Mejnertsen, L., Eastwood, J. P., Chittenden, J. P., et al. (2016), Global MHD simulations of Neptune's
1428 magnetosphere, *Journal of Geophysical Research (Space Physics)*, 121, 7497, 10.1002/2015JA022272.
- 1429
- 1430 Melin, H., Stallard, T., Miller, S., et al. (2011), Seasonal Variability in the Ionosphere of Uranus, *The*
1431 *Astrophysical Journal*, 729, 134, 10.1088/0004-637X/729/2/134.
- 1432
- 1433 Melin, H., Fletcher, L. N., Stallard, T. S., et al. (2019), The H₃⁺ ionosphere of Uranus: decades-long cooling
1434 and local-time morphology, *Philosophical Transactions of the Royal Society of London Series A*, 377,
1435 20180408, 10.1098/rsta.2018.0408.
- 1436
- 1437 Melin, H., Stallard, T. S., Miller, S., et al. (2013), Post-equinoctial observations of the ionosphere of Uranus,
1438 *Icarus*, 223, 741, 10.1016/j.icarus.2013.01.012.
- 1439

- 1440 Merrill, R. T., & McFadden, P. L. (1999), Geomagnetic polarity transitions, *Reviews of Geophysics*, 37, 201,
1441 10.1029/1998RG900004.
- 1442
- 1443 Millot, M., Coppari, F., Rygg, J. R., et al. (2019), Nanosecond X-ray diffraction of shock-compressed
1444 superionic water ice, *Nature*, 569, 251, 10.1038/s41586-019-1114-6.
- 1445
- 1446 Molter, E. M., de Pater, I., Roman, M. T., et al. (2019), Thermal Emission from the Uranian Ring System, *The*
1447 *Astronomical Journal*, 158, 47, 10.3847/1538-3881/ab258c.
- 1448
- 1449 Moreno, R., Marten, A., & Lellouch, E. (2009), Search for PH₃ in the Atmospheres of Uranus and Neptune at
1450 Millimeter Wavelength, *AAS/Division for Planetary Sciences Meeting Abstracts #41*, 28.02.
- 1451
- 1452 Morley, C. V., Fortney, J. J., Marley, M. S., et al. (2012), Neglected Clouds in T and Y Dwarf Atmospheres,
1453 *The Astrophysical Journal*, 756, 172, 10.1088/0004-637X/756/2/172.
- 1454
- 1455 Moses, J. I., & Poppe, A. R. (2017), Dust ablation on the giant planets: Consequences for stratospheric
1456 photochemistry, *Icarus*, 297, 33, 10.1016/j.icarus.2017.06.002.
- 1457
- 1458 Moses, J. I., Fletcher, L. N., Greathouse, T. K., et al. (2018), Seasonal stratospheric photochemistry on
1459 Uranus and Neptune, *Icarus*, 307, 124, 10.1016/j.icarus.2018.02.004.
- 1460
- 1461 Mousis, O., Atkinson, D. H., Cavalié, T., et al. (2018), Scientific rationale for Uranus and Neptune in situ
1462 explorations, *Planetary and Space Science*, 155, 12, 10.1016/j.pss.2017.10.005.
- 1463
- 1464 Namouni, F., & Porco, C. (2002), The confinement of Neptune's ring arcs by the moon Galatea, *Nature*, 417,
1465 45, 10.1038/417045a.

1466

1467 Nettelman, N., Helled, R., Fortney, J. J., et al. (2013), New indication for a dichotomy in the interior
1468 structure of Uranus and Neptune from the application of modified shape and rotation data, *Planetary and*
1469 *Space Science*, 77, 143, 10.1016/j.pss.2012.06.019.

1470

1471 Neubauer, F. M. (1990), Satellite plasma interactions, *Advances in Space Research*, 10, 25, 10.1016/0273-
1472 1177(90)90083-C.

1473

1474 Nicholson, P. D., De Pater, I., French, R. G., et al. (2018), The Rings of Uranus, *Planetary Ring Systems.*
1475 *Properties, Structure, and Evolution*, 93, 10.1017/9781316286791.004.

1476

1477 Nimmo, F., & Spencer, J. R. (2015), Powering Triton's recent geological activity by obliquity tides:
1478 Implications for Pluto geology, *Icarus*, 246, 2, 10.1016/j.icarus.2014.01.044.

1479

1480 Orton, G. S., Fletcher, L. N., Moses, J. I., et al. (2014), Mid-infrared spectroscopy of Uranus from the Spitzer
1481 Infrared Spectrometer: 1. Determination of the mean temperature structure of the upper troposphere and
1482 stratosphere, *Icarus*, 243, 494, 10.1016/j.icarus.2014.07.010.

1483

1484 Pearl, J. C., Conrath, B. J., Hanel, R. A., et al. (1990), The albedo, effective temperature, and energy balance
1485 of Uranus, as determined from Voyager IRIS data, *Icarus*, 84, 12, 10.1016/0019-1035(90)90155-3.

1486

1487 Pearl, J. C., & Conrath, B. J. (1991), The albedo, effective temperature, and energy balance of Neptune, as
1488 determined from Voyager data, *Journal of Geophysical Research*, 96, 18921, 10.1029/91JA01087.

1489

1490 Penny, M. T., Gaudi, B. S., Kerins, E., et al. (2019), Predictions of the WFIRST Microlensing Survey. I. Bound
1491 Planet Detection Rates, *The Astrophysical Journal Supplement Series*, 241, 3, 10.3847/1538-4365/aafb69.

1492

1493 Petigura, E. A., Howard, A. W., Marcy, G. W., et al. (2017), The California-Kepler Survey. I. High-resolution
1494 Spectroscopy of 1305 Stars Hosting Kepler Transiting Planets, *The Astronomical Journal*, 154, 107,
1495 10.3847/1538-3881/aa80de.

1496

1497 Plainaki, C., Lilensten, J., Radioti, A., et al. (2016), Planetary space weather: scientific aspects and future
1498 perspectives, *Journal of Space Weather and Space Climate*, 6, A31, 10.1051/swsc/2016024.

1499

1500 Plescia, J. B. (1987a), Cratering history of the Uranian satellites: Umbriel, Titania, and Oberon, *Journal of*
1501 *Geophysical Research*, 92, 14918, 10.1029/JA092iA13p14918.

1502

1503 Plescia, J. B. (1987b), Geological terrains and crater frequencies on Ariel, *Nature*, 327, 201,
1504 10.1038/327201a0.

1505

1506 Podolak, M., & Helled, R. (2012), What Do We Really Know about Uranus and Neptune?, *The Astrophysical*
1507 *Journal*, 759, L32, 10.1088/2041-8205/759/2/L32.

1508

1509 Podolak, M., Weizman, A., & Marley, M. (1995), Comparative models of Uranus and Neptune, *Planetary*
1510 *and Space Science*, 43, 1517, 10.1016/0032-0633(95)00061-5.

1511

1512 Pollack, J. B., Hubickyj, O., Bodenheimer, P., et al. (1996), Formation of the Giant Planets by Concurrent
1513 Accretion of Solids and Gas, *Icarus*, 124, 62, 10.1006/icar.1996.0190.

1514

1515 Postberg, F., Kempf, S., Schmidt, J., et al. (2009), Sodium salts in E-ring ice grains from an ocean below the
1516 surface of Enceladus, *Nature*, 459, 1098, 10.1038/nature08046.

1517

- 1518 Prockter, L. M., Nimmo, F., & Pappalardo, R. T. (2005), A shear heating origin for ridges on Triton,
1519 Geophysical Research Letters, 32, L14202, 10.1029/2005GL022832.
- 1520
- 1521 Quirico, E., Douté, S., Schmitt, B., et al. (1999), Composition, Physical State, and Distribution of Ices at the
1522 Surface of Triton, Icarus, 139, 159, 10.1006/icar.1999.6111.
- 1523
- 1524 Rages, K., Pollack, J. B., Tomasko, M. G., et al. (1991), Properties of scatterers in the troposphere and lower
1525 stratosphere of Uranus based on Voyager imaging data, Icarus, 89, 359, 10.1016/0019-1035(91)90183-T.
- 1526
- 1527 Redmer, R., Mattsson, T. R., Nettelmann, N., et al. (2011), The phase diagram of water and the magnetic
1528 fields of Uranus and Neptune, Icarus, 211, 798, 10.1016/j.icarus.2010.08.008.
- 1529
- 1530 Reinhardt, C., Chau, A., Stadel, J., et al. (2020), Bifurcation in the history of Uranus and Neptune: the role of
1531 giant impacts, Monthly Notices of the Royal Astronomical Society, 492, 5336, 10.1093/mnras/stz3271.
- 1532
- 1533 Richardson, J. D., & McNutt, R. L. (1990), Low-energy plasma in Neptune's magnetosphere, Geophysical
1534 Research Letters, 17, 1689, 10.1029/GL017i010p01689.
- 1535
- 1536 Roman, M. T., Fletcher, L. N., Orton, G. S., et al. (2020), Uranus in Northern Midspring: Persistent
1537 Atmospheric Temperatures and Circulations Inferred from Thermal Imaging, The Astronomical Journal, 159,
1538 45, 10.3847/1538-3881/ab5dc7.
- 1539
- 1540 Rymer, A., Mandt, K., Hurley, D., et al. (2019), Solar System Ice Giants: Exoplanets in our Backyard., Bulletin
1541 of the American Astronomical Society, 51, 176.
- 1542

- 1543 Safronov, V. S. (1966), Sizes of the largest bodies falling onto the planets during their formation, Soviet
1544 Astronomy, 9, 987.
- 1545
- 1546 Sánchez-Lavega, A., Sromovsky, L. A., et al. (2018), Gas Giants. In: Galperin, B., Read, P.L., (eds) Zonal Jets
1547 Phenomenology, Genesis and Physics. Cambridge (doi: 10.1017/9781107358225).
- 1548
- 1549 Scarf, F. L., Gurnett, D. A., Kurth, W. S., et al. (1987), Voyager 2 plasma wave observations at Uranus,
1550 Advances in Space Research, 7, 253, 10.1016/0273-1177(87)90226-2.
- 1551
- 1552 Selesnick, R. S. (1988), Magnetospheric convection in the nondipolar magnetic field of Uranus, Journal of
1553 Geophysical Research, 93, 9607, 10.1029/JA093iA09p09607.
- 1554
- 1555 Showalter, M. R., & Lissauer, J. J. (2006), The Second Ring-Moon System of Uranus: Discovery and
1556 Dynamics, Science, 311, 973, 10.1126/science.1122882.
- 1557
- 1558 Simon, A. A., Fletcher, L. N., Arridge, C., et al. (2020), A Review of the in Situ Probe Designs from Recent Ice
1559 Giant Mission Concept Studies, Space Science Reviews, 216, 17, 10.1007/s11214-020-0639-1.
- 1560
- 1561 Simon, A. A., Wong, M. H., & Hsu, A. I. (2019), Formation of a New Great Dark Spot on Neptune in 2018,
1562 Geophysical Research Letters, 46, 3108, 10.1029/2019GL081961.
- 1563
- 1564 Simon, A. A., Stern, S. A., & Hofstadter, M. (2018), Outer Solar System Exploration: A Compelling and
1565 Unified Dual Mission Decadal Strategy for Exploring Uranus, Neptune, Triton, Dwarf Planets, and Small
1566 KBOs and Centaurs, arXiv e-prints, arXiv:1807.08769.
- 1567

- 1568 Simon, A. A., Rowe, J. F., Gaulme, P., et al. (2016), Neptune's Dynamic Atmosphere from Kepler K2
1569 Observations: Implications for Brown Dwarf Light Curve Analyses, *The Astrophysical Journal*, 817, 162,
1570 10.3847/0004-637X/817/2/162.
- 1571
- 1572 Slattery, W. L., Benz, W., & Cameron, A. G. W. (1992), Giant impacts on a primitive Uranus, *Icarus*, 99, 167,
1573 10.1016/0019-1035(92)90180-F.
- 1574
- 1575 Smith, B. A., Soderblom, L. A., Banfield, D., et al. (1989), Voyager 2 at Neptune: Imaging Science Results,
1576 *Science*, 246, 1422, 10.1126/science.246.4936.1422.
- 1577
- 1578 Smith, M. D., & Gierasch, P. J. (1995), Convection in the outer planet atmospheres including ortho-para
1579 hydrogen conversion., *Icarus*, 116, 159, 10.1006/icar.1995.1118.
- 1580
- 1581 Soderblom, L. A., Kieffer, S. W., Becker, T. L., et al. (1990), Triton's Geyser-Like Plumes: Discovery and Basic
1582 Characterization, *Science*, 250, 410, 10.1126/science.250.4979.410.
- 1583
- 1584 Soderlund, K. M., Heimpel, M. H., King, E. M., et al. (2013), Turbulent models of ice giant internal dynamics:
1585 Dynamos, heat transfer, and zonal flows, *Icarus*, 224, 97, 10.1016/j.icarus.2013.02.014.
- 1586
- 1587 Sromovsky, L. A., de Pater, I., Fry, P. M., et al. (2015), High S/N Keck and Gemini AO imaging of Uranus
1588 during 2012-2014: New cloud patterns, increasing activity, and improved wind measurements, *Icarus*, 258,
1589 192, 10.1016/j.icarus.2015.05.029.
- 1590
- 1591 Sromovsky, L. A., Karkoschka, E., Fry, P. M., et al. (2014), Methane depletion in both polar regions of Uranus
1592 inferred from HST/STIS and Keck/NIRC2 observations, *Icarus*, 238, 137, 10.1016/j.icarus.2014.05.016.
- 1593

- 1594 Stanley, S., & Bloxham, J. (2004), Convective-region geometry as the cause of Uranus' and Neptune's
1595 unusual magnetic fields, *Nature*, 428, 151, 10.1038/nature02376.
- 1596
- 1597 Stanley, S., & Bloxham, J. (2006), Numerical dynamo models of Uranus' and Neptune's magnetic fields,
1598 *Icarus*, 184, 556, 10.1016/j.icarus.2006.05.005.
- 1599
- 1600 Stauffer, J., Marley, M. S., Gizis, J. E., et al. (2016), Spitzer Space Telescope Mid-IR Light Curves of Neptune,
1601 *The Astronomical Journal*, 152, 142, 10.3847/0004-6256/152/5/142.
- 1602
- 1603 Stern, S. A., & McKinnon, W. B. (2000), Triton's Surface Age and Impactor Population Revisited in Light of
1604 Kuiper Belt Fluxes: Evidence for Small Kuiper Belt Objects and Recent Geological Activity, *The Astronomical*
1605 *Journal*, 119, 945, 10.1086/301207.
- 1606
- 1607 Stevenson, D. J. (1986), The Uranus-Neptune Dichotomy: the Role of Giant Impacts, *Lunar and Planetary*
1608 *Science Conference*, 1011.
- 1609
- 1610 Stoker, C. R., & Toon, O. B. (1989), Moist convection on Neptune, *Geophysical Research Letters*, 16, 929,
1611 10.1029/GL016i008p00929.
- 1612
- 1613 Stone, E. C., Cooper, J. F., Cummings, A. C., et al. (1986), Energetic Charged Particles in the Uranian
1614 Magnetosphere, *Science*, 233, 93, 10.1126/science.233.4759.93.
- 1615
- 1616 Stratman, P. W., Showman, A. P., Dowling, T. E., et al. (2001), EPIC Simulations of Bright Companions to
1617 Neptune's Great Dark Spots, *Icarus*, 151, 275, 10.1006/icar.2001.6603.
- 1618

- 1619 Strobel, D. F., Cheng, A. F., Summers, M. E., et al. (1990), Magnetospheric interaction with Triton's
1620 ionosphere, *Geophysical Research Letters*, 17, 1661, 10.1029/GL017i010p01661.
- 1621
- 1622 Stryk, T., & Stooke, P. J. (2008), Voyager 2 Images of Uranian Satellites: Reprocessing and New
1623 Interpretations, *Lunar and Planetary Science Conference*, 1362.
- 1624
- 1625 Sun, Z.-P., Schubert, G., & Stoker, C. R. (1991), Thermal and humidity winds in outer planet atmospheres,
1626 *Icarus*, 91, 154, 10.1016/0019-1035(91)90134-F.
- 1627
- 1628 Tegler, S. C., Grundy, W. M., Olkin, C. B., et al. (2012), Ice Mineralogy across and into the Surfaces of Pluto,
1629 Triton, and Eris, *The Astrophysical Journal*, 751, 76, 10.1088/0004-637X/751/1/76.
- 1630
- 1631 Tegler, S. C., Stufflebeam, T. D., Grundy, W. M., et al. (2019), A New Two-molecule Combination Band as a
1632 Diagnostic of Carbon Monoxide Diluted in Nitrogen Ice on Triton, *The Astronomical Journal*, 158, 17,
1633 10.3847/1538-3881/ab199f.
- 1634
- 1635 Thompson, W. R., & Sagan, C. (1990), Color and chemistry on Triton, *Science*, 250, 415,
1636 10.1126/science.11538073.
- 1637
- 1638 Tiscareno, M. S., Hedman, M. M., Burns, J. A., et al. (2013), Compositions and Origins of Outer Planet
1639 Systems: Insights from the Roche Critical Density, *The Astrophysical Journal*, 765, L28, 10.1088/2041-
1640 8205/765/2/L28.
- 1641
- 1642 Titemore, W. C., & Wisdom, J. (1990), Tidal evolution of the Uranian satellites III. Evolution through the
1643 Miranda-Umbriel 3:1, Miranda-Ariel 5:3, and Ariel-Umbriel 2:1 mean-motion commensurabilities, *Icarus*,
1644 85, 394, 10.1016/0019-1035(90)90125-S.

1645

1646 Tosi, F., Turrini, D., Coradini, A., et al. (2010), Probing the origin of the dark material on Iapetus, Monthly
1647 Notices of the Royal Astronomical Society, 403, 1113, 10.1111/j.1365-2966.2010.16044.x.

1648

1649 Turrini, D., Politi, R., Peron, R., et al. (2014), The comparative exploration of the ice giant planets with twin
1650 spacecraft: Unveiling the history of our Solar System, Planetary and Space Science, 104, 93,
1651 10.1016/j.pss.2014.09.005.

1652

1653 Venturini, J., & Helled, R. (2017), The Formation of Mini-Neptunes, The Astrophysical Journal, 848, 95,
1654 10.3847/1538-4357/aa8cd0.

1655

1656 Waite, J. H., Perryman, R. S., Perry, M. E., et al. (2018), Chemical interactions between Saturn's atmosphere
1657 and its rings, Science, 362, aat2382, 10.1126/science.aat2382.

1658

1659 Wakeford, H. R., Visscher, C., Lewis, N. K., et al. (2017), High-temperature condensate clouds in super-hot
1660 Jupiter atmospheres, Monthly Notices of the Royal Astronomical Society, 464, 4247,
1661 10.1093/mnras/stw2639.

1662

1663 Wang, C., & Richardson, J. D. (2004), Interplanetary coronal mass ejections observed by Voyager 2 between
1664 1 and 30 AU, Journal of Geophysical Research (Space Physics), 109, A06104, 10.1029/2004JA010379.

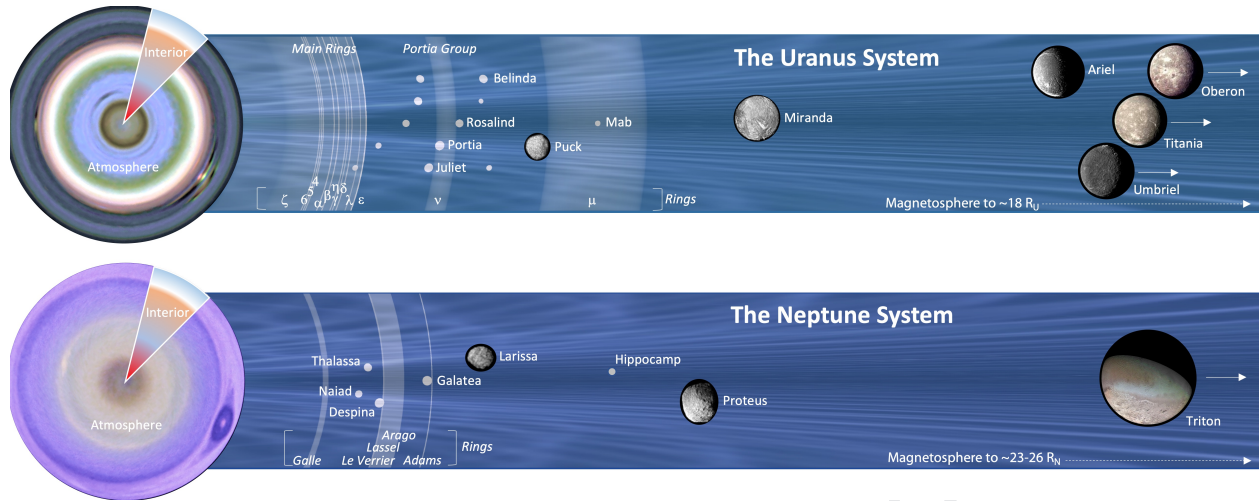
1665

1666 Wei, Y., Pu, Z., Zong, Q., et al. (2014), Oxygen escape from the Earth during geomagnetic reversals:
1667 Implications to mass extinction, Earth and Planetary Science Letters, 394, 94, 10.1016/j.epsl.2014.03.018.

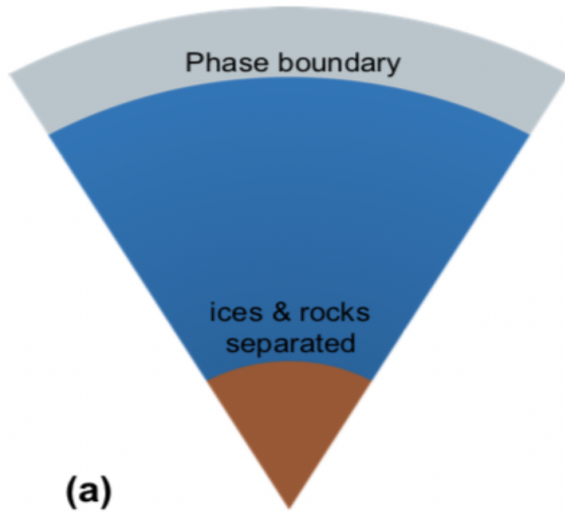
1668

1669 Witasse, O., Sánchez-Cano, B., Mays, M. L., et al. (2017), Interplanetary coronal mass ejection observed at
1670 STEREO-A, Mars, comet 67P/Churyumov-Gerasimenko, Saturn, and New Horizons en route to Pluto:

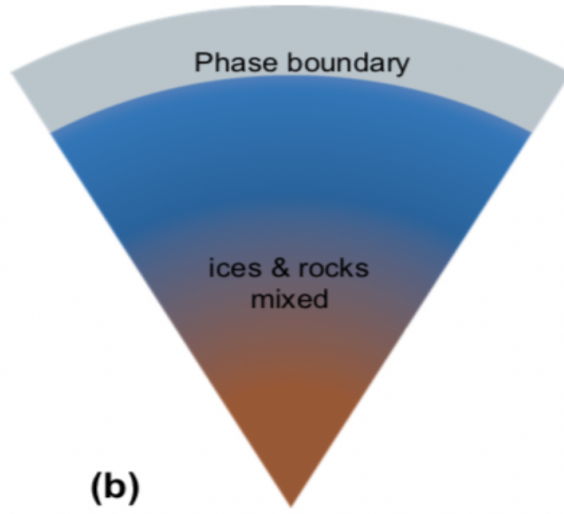
- 1671 Comparison of its Forbush decreases at 1.4, 3.1, and 9.9 AU, *Journal of Geophysical Research (Space*
1672 *Physics)*, 122, 7865, 10.1002/2017JA023884.
- 1673
- 1674 Wong, M. H., Tollefson, J., Hsu, A. I., et al. (2018), A New Dark Vortex on Neptune, *The Astronomical*
1675 *Journal*, 155, 117, 10.3847/1538-3881/aaa6d6.
- 1676
- 1677 Zarka, P., & Pedersen, B. M. (1986), Radio detection of uranian lightning by Voyager 2, *Nature*, 323, 605,
1678 10.1038/323605a0.
- 1679
- 1680 Zarka, P., Pedersen, B. M., Lecacheux, A., et al. (1995), Radio emissions from Neptune., *Neptune and Triton*,
1681 341.
- 1682
- 1683 Zhang, Z., Hayes, A. G., Janssen, M. A., et al. (2017), Exposure age of Saturn's A and B rings, and the Cassini
1684 Division as suggested by their non-icy material content, *Icarus*, 294, 14, 10.1016/j.icarus.2017.04.008.
- 1685
- 1686



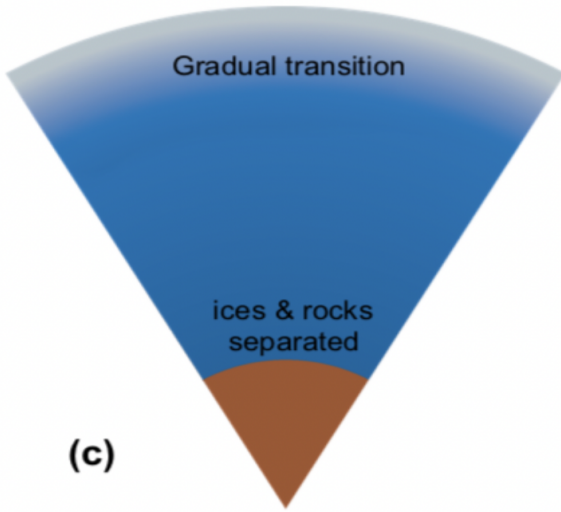
Journal Pre-proof



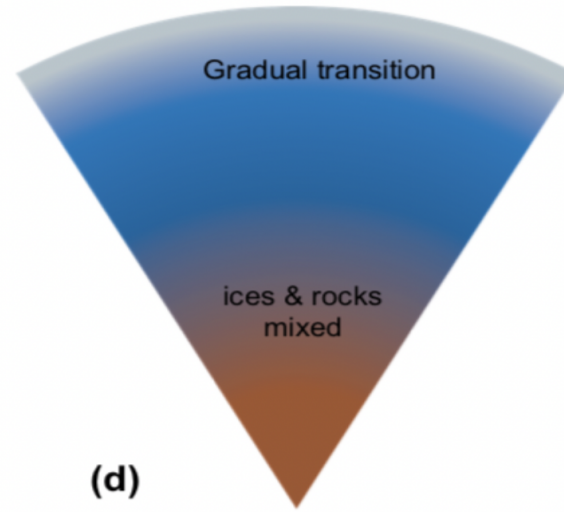
(a)



(b)

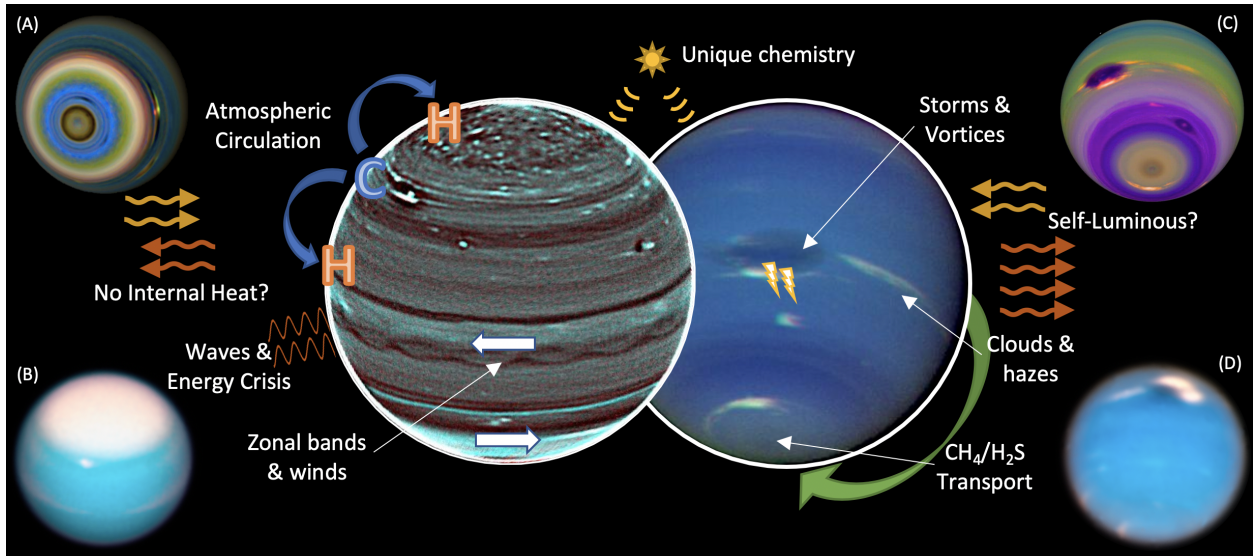


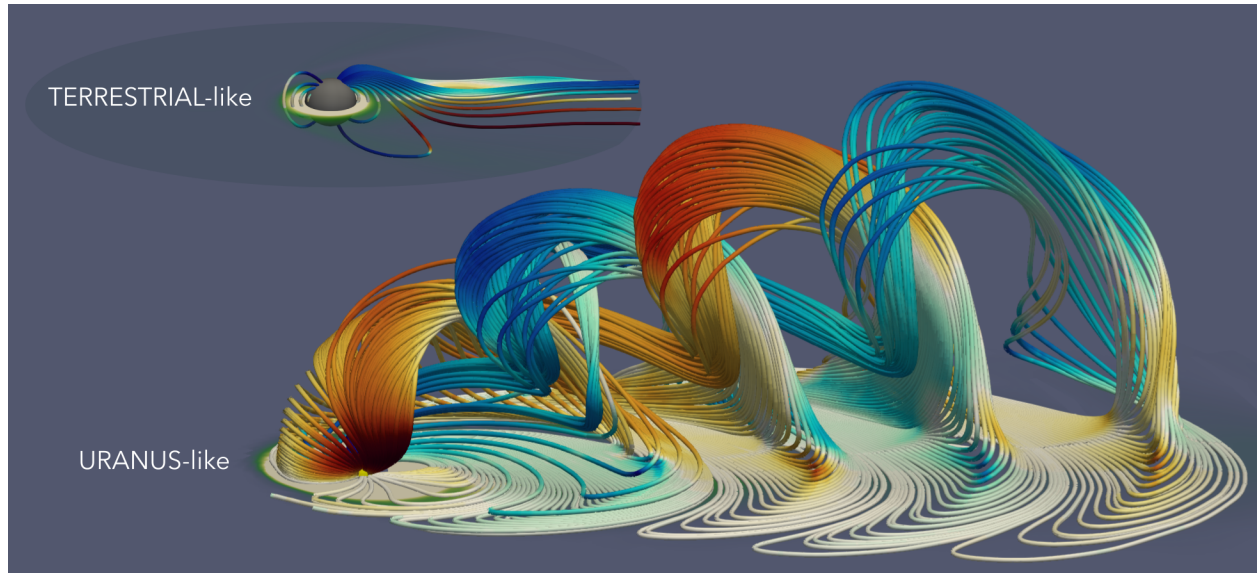
(c)



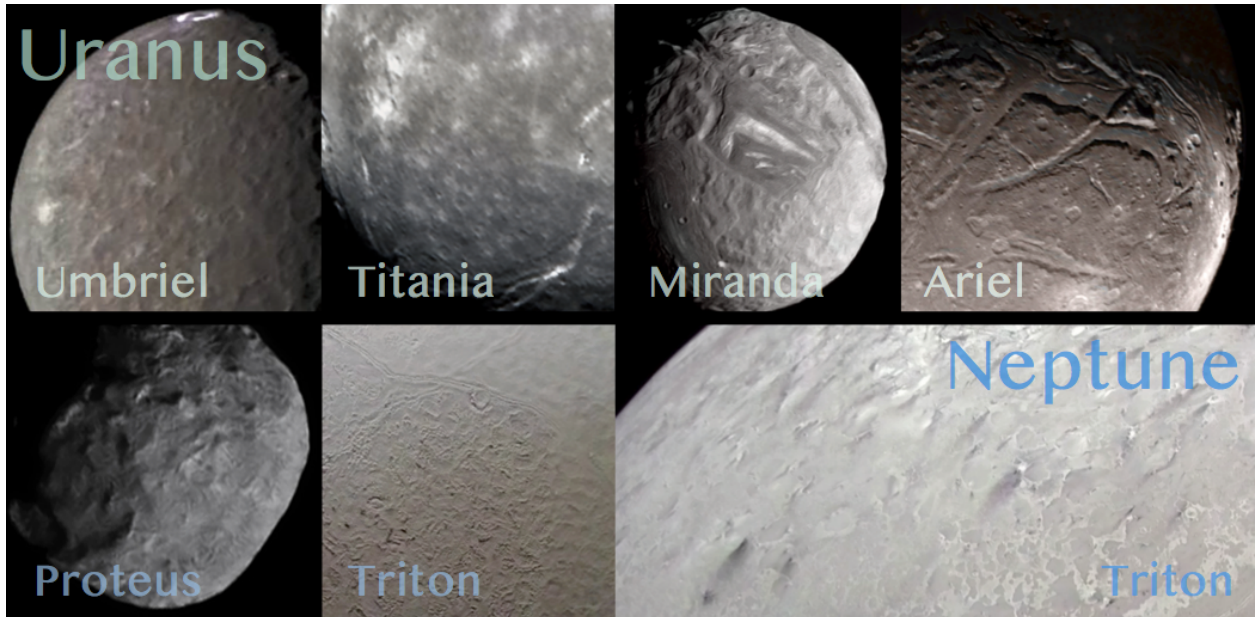
(d)

JU

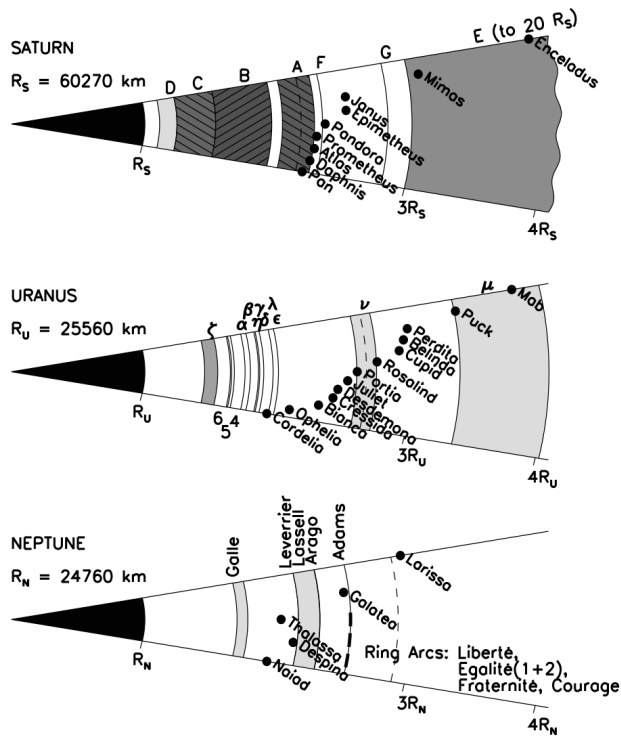




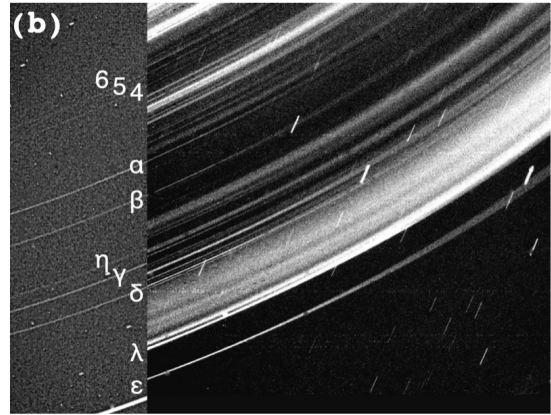
Journal Pre-proof



(a)



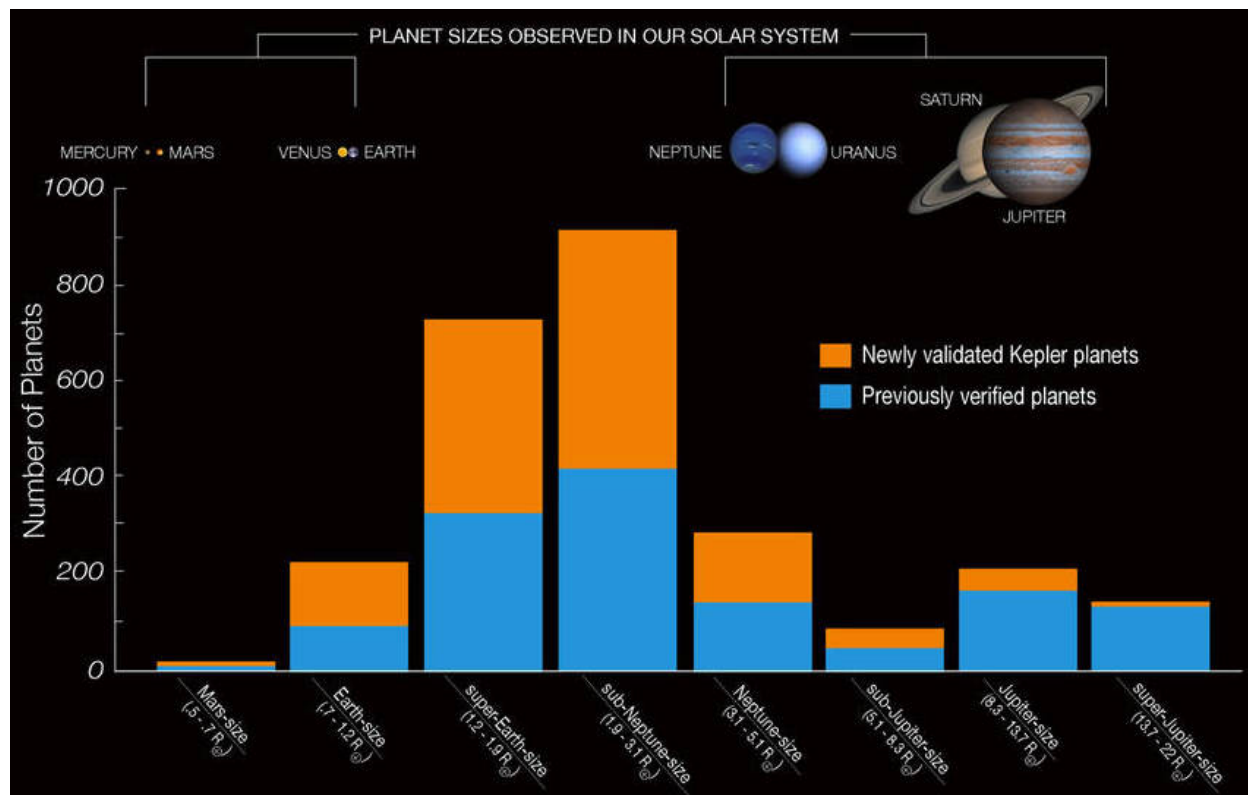
(b)



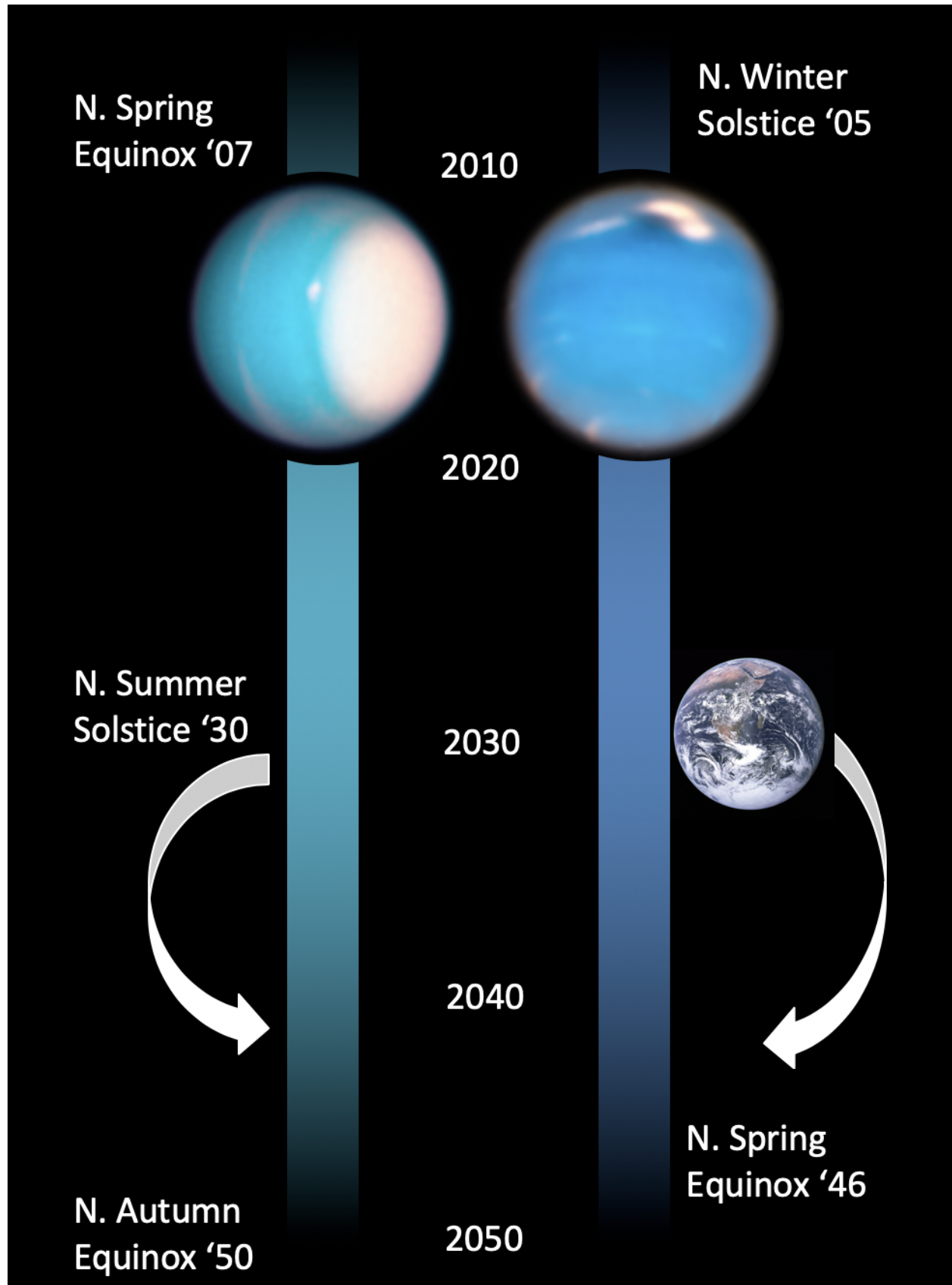
(c)

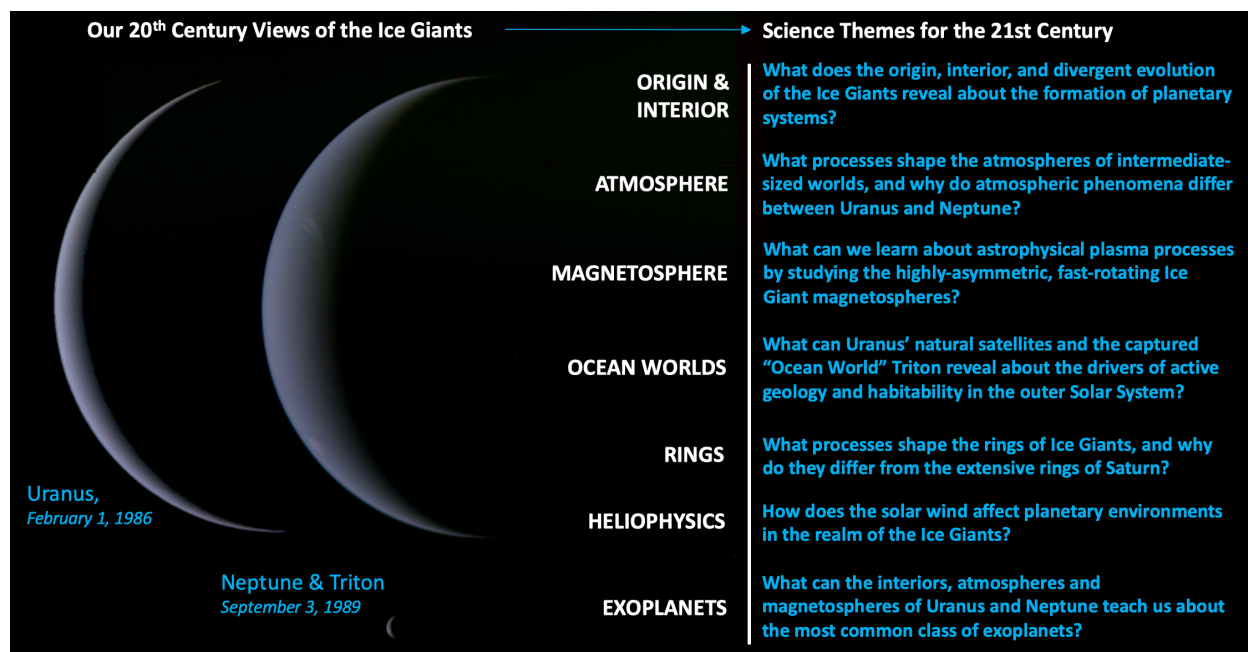


Journal



Journal Pre-proof





Journal Pre-proof

Declaration of interests

The authors declare that they have no known competing financial interests or personal relationships that could have appeared to influence the work reported in this paper.

The authors declare the following financial interests/personal relationships which may be considered as potential competing interests:

Journal Pre-proof